# Chapter 1

# The Two Dimensional Fully Frustrated XY Model

Stephen Teitel
*Department of Physics and Astronomy*
*University of Rochester*
*Rochester, NY 14627*

In this chapter we discuss the two dimensional uniformly frustrated XY model, which arises as a model for a periodic array of Josephson junctions in an applied magnetic field. We will focus primarily on the fully frustrated model, which exhibits both phase angle ordering of the XY spins as well as a discrete $Z_2$ ordering corresponding to the spatial structure of vortices in the ground state of the model.

## 1.1. Introduction

The seminal works of Berezinskii [1, 2] and of Kosterlitz and Thouless [3, 4] on the role of topological excitations in mediating continuous phase transitions has found wide application to numerous physical systems. In this chapter we discuss a class of classical two dimensional statistical models, known as the uniformly frustrated XY model, which serves as a model for describing behavior in a planar periodic array of Josephson junctions in a perpendicular applied magnetic field. We will focus primarily on the specific case known as the fully frustrated XY model (FFXY). We will show how the ideas of Berezinskii and of Kosterlitz and Thouless are crucial for an understanding of behavior in the FFXY, and we will make use of them in two different contexts: first, in arguing about the lose of phase angle coherence in the model due to a vortex-antivortex unbinding transition, and second, in discussing a kink-antikink transition that takes place along the domain walls separating regions of different discrete symmetry in the system. We will discuss the intimate connection that exists between these two different phenomena.

## 1.2. The Uniformly Frustrated XY Model

The Hamiltonian for the ordinary two dimensional (2D) XY model on a square lattice is,

$$\mathcal{H} = -J \sum_{i\mu} \mathbf{S}(\mathbf{r}_i) \cdot \mathbf{S}(\mathbf{r}_i + \hat{\mu}) \ . \tag{1.1}$$

Here $\mathbf{S}(\mathbf{r}_i)$ is a planar spin of unit magnitude on site $\mathbf{r}_i = (x, y)$ of a square lattice, the sum is over nearest neighbor bonds in directions $\hat{\mu} = \hat{x}, \hat{y}$, and $J > 0$ is the ferromagnetic coupling constant. We will take the coordinates $x$ and $y$ as integers.

If one represents the spin $\mathbf{S}(\mathbf{r}_i)$ in terms the angle $\theta(\mathbf{r}_i)$ it makes with respect to some fixed direction, then the Hamiltonian (1.1) can be rewritten as,

$$\mathcal{H} = -J \sum_{i\mu} \cos(\theta(\mathbf{r}_i + \hat{\mu}) - \theta(\mathbf{r}_i)) \ . \tag{1.2}$$

The latter expression for the Hamiltonian suggests a particular physical application of the model. If we regard the nodes of our lattice as superconducting islands, with $\theta(\mathbf{r}_i)$ the phase angle of the superconducting wavefunction on island $i$, $\psi(\mathbf{r}_i) = |\psi| e^{i\theta(\mathbf{r}_i)}$, then Eq. (1.2) becomes the Hamiltonian for an array of Josephson junctions, with one junction on each bond of the lattice [5–7].

This mapping to a Josephson junction array then suggests an interesting generalization of the XY model. The Hamiltonian (1.2) represents a Josephson junction array in the absence of any applied magnetic field. If a magnetic field is applied, we must modify Eq. (1.2) so that the phase angle difference becomes the *gauge invariant* phase angle difference between neighboring nodes,

$$\mathcal{H} = -J \sum_{i\mu} \cos(\theta(\mathbf{r}_i + \hat{\mu}) - \theta(\mathbf{r}_i) - A_\mu(\mathbf{r}_i)) \ , \tag{1.3}$$

where

$$A_\mu(\mathbf{r}_i) \equiv \frac{2\pi}{\Phi_0} \int_{\mathbf{r}_i}^{\mathbf{r}_i + \hat{\mu}} \mathbf{A} \cdot \ell \tag{1.4}$$

is proportional to the line integral of the magnetic vector potential $\mathbf{A}$ across the bond at note $i$ in direction $\hat{\mu}$, and $\Phi_0 = hc/2e$ is the flux quantum. The sum of the $A_\mu(\mathbf{r}_i)$ going counterclockwise around any closed path $C$ of bonds on the lattice is $2\pi$ times the number of magnetic flux quanta $f_C$ penetrating the path,

$$\sum_C A_\mu(\mathbf{r}_i) = \frac{2\pi}{\Phi_0} \oint_C \mathbf{A} \cdot \ell = 2\pi \frac{\Phi_C}{\Phi_0} \equiv 2\pi f_C \tag{1.5}$$

where $\Phi_C$ is the total magnetic flux through the path $C$. In Fig. 1.1 the geometry of such a Josephson junction array is illustrated.

The addition of the phase factor $A_\mu(\mathbf{r}_i)$ to the argument of the cosine in Eq. (1.3) adds *frustration* to the system; in general, the ground state will no longer be ferromagnetic with all $\theta(\mathbf{r}_i)$ equal, but rather the $\theta(\mathbf{r}_i)$ will vary from node to node so as to try and minimize the gauge invariant phase angle difference $\theta(\mathbf{r}_i + \hat{\mu}) - \theta(\mathbf{r}_i) - A_\mu(\mathbf{r}_i)$ across the bonds. Depending on the values of the $A_\mu(\mathbf{r}_i)$, the ground state can develop inhomogeneous spatial structure.

For the case of a uniform magnetic field $H$ applied perpendicular to the plane of the array, the number $f$ of flux quanta per unit cell of the square array is constant, and Eq. (1.3) is known as the *uniformly frustrated* XY model with uniform frustration $f$ [8, 9]. The ground state of the system now consists of a periodic

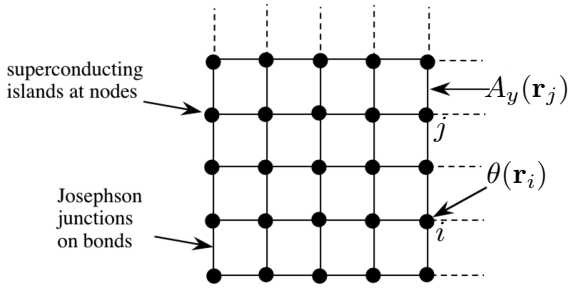


Fig. 1.1. Schematic geometry of the square lattice Josephson junction array with Hamiltonian as in Eq. (1.3).

configuration of vortices in the phase angle $\theta(\mathbf{r}_i)$, similar to the Abrikosov vortex lattice in a type-II superconductor. However, whereas in a homogeneous continuous superconductor the Abrikosov vortex lattice is is always triangular, in the Josephson array vortices are constrained to sit at the centers of the unit cells of the array lattice. The result, in general, is a nontrivial spatial structure for the vortices that results from a competition between vortex-vortex repulsion and commensurability with the geometry of the Josephson array. In Fig. 1.2 are shown the ground state vortex structures for several simple rational fractions $f$.

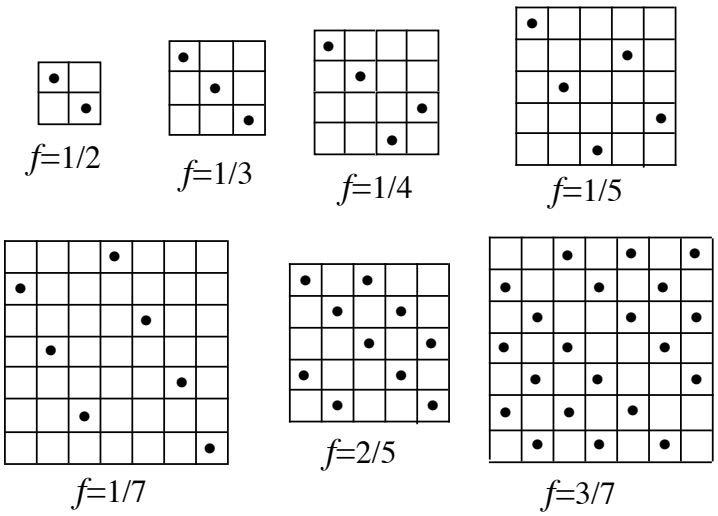


Fig. 1.2. Ground state vortex structures for several simple rational fractions of the uniform frustration $f$. The ground state is given by the periodic tiling of space with the shown structure. Solid dots indicate the location of vortices in the phase angle $\theta(\mathbf{r}_i)$.

A convenient choice of gauge for representing the uniform frustration $f$ is to take,

$$A_\mu(\mathbf{r}_i) = \begin{cases} 2\pi f y & \mu = x, \text{ i.e. on horizontal bonds} \\ 0 & \mu = y, \text{ i.e. on vertical bonds} \end{cases} \tag{1.6}$$

If we now take $f \to f + 1$, we see that the $A_\mu(\mathbf{r}_i)$ on the horizontal bonds change by integral multiples of $2\pi$, leaving the Hamiltonian (1.3) invariant. It is thus only necessary to consider $f$ in the range of $-1/2$ to $+1/2$.

### 1.3. The Fully Frustrated XY Model

The main focus of this article will be the special case $f = 1/2$. In this case, using the gauge choice of Eq. (1.6), the horizontal bonds take values 0 and $\pi$ (modulus $2\pi$) on alternating rows of bonds. For the Hamiltonian (1.3), bonds with $A_\mu(\mathbf{r}_i) = \pi$ become antiferromagnetic bonds, as $J\cos(\varphi - \pi) = -J\cos(\varphi)$. As the product of bonds around any unit cell of the array is always negative, this model is known as the *fully frustrated* XY model (FFXY) [10, 11].

In Fig. 1.3 we show ground state configurations for the FFXY model. The gauge invariant phase angle difference across all bonds is $\pi/4$, as shown in the top row of Fig. 1.3. As in the ordinary XY model, rotating all spins, $\theta(\mathbf{r}_i) \to \theta(\mathbf{r}_i) + \theta_0$ with $\theta_0$ a constant, leaves the Hamiltonian (1.3) invariant. The ground state breaks this continuous symmetry $U(1)$ by picking out a particular direction for the spins. However the particular spatial structure of the ground state also leads to the breaking of a discrete two-fold symmetry $Z_2$. This is most readily seen in the "charge" representation.

Let us denote the gauge invariant phase angle difference across the bond leaving node $i$ in direction $\hat{\mu}$ by,

$$\varphi_\mu(\mathbf{r}_i) \equiv [\theta(\mathbf{r}_i + \hat{\mu}) - \theta(\mathbf{r}_i) - A_\mu(\mathbf{r}_i)]_{-\pi}^{\pi} \tag{1.7}$$

where the notation $[\dots]_{-\pi}^{\pi}$ means that we take the value modulus $2\pi$ so that it lies in the interval $(-\pi, \pi]$. For simplicity of notation, we will denote a unit cell (plaquette) of the array by the position $\mathbf{r}_i$ of the node at the cell's lower left corner. We can then compute the circulation of the gauge invariant phase going counterclockwise around the unit cell at $\mathbf{r}_i$,

$$\varphi_x(\mathbf{r}_i) + \varphi_y(\mathbf{r}_i + \hat{x}) - \varphi_x(\mathbf{r}_i + \hat{y}) - \varphi_y(\mathbf{r}_i) = 2\pi(n_i - f) \equiv 2\pi q_i \ , \tag{1.8}$$

where $n_i$ is the integer vorticity in the phase angle $\theta(\mathbf{r}_i)$ going around the unit cell at $\mathbf{r}_i$, and $f$ is the uniform frustration, with $f = 1/2$ for the fully frustrated model. At low temperatures, the vorticity will take only the values $n_i = 0, +1$, leading to charges $q_i = \pm 1/2$. This charge analogy will be pursued in greater detail in a following section. Here we just note that at low temperature one finds only configurations with equal numbers of $+1/2$ and $-1/2$ charges. In the ground state, these charges are arranged in a checkerboard pattern, as shown in the bottom row

of Fig. 1.3, with two possibilities for the sub-lattice on which to put the positive charges. Taking $q_i \to -q_i$ is then a discrete symmetry of the Hamiltonian (1.3) that is broken in the ground state.

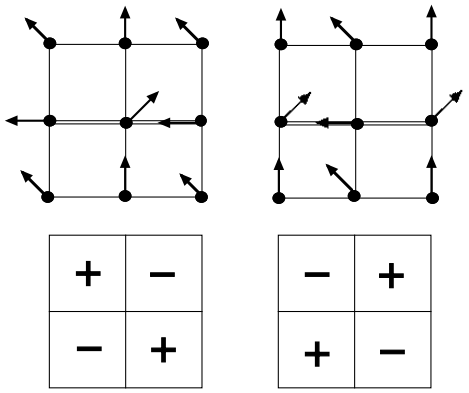


Fig. 1.3. Ground states of the fully frustrated XY model. Top: arrows denote spin directions, giving the phase angles $\theta(\mathbf{r}_i)$; double horizontal line denotes the antiferromagnetic bonds, where $A_\mu(\mathbf{r}_i) = \pi$. Bottom: corresponding charge configurations with $q_i = \pm 1/2$.

The ground state of the FFXY model thus breaks both continuous $U(1)$ and discrete $Z_2$ symmetries. A main question of interest is whether, upon cooling, these two different symmetries are broken at the same or different temperatures.

### 1.3.1. *Phase Angle Ordering*

Just as in the ordinary XY model, one can consider smooth perturbations about the ground state to describe the low lying excitations of the system; this is the *spinwave approximation*. Writing $\theta(\mathbf{r}_i) = \theta_0(\mathbf{r}_i) + \delta\theta(\mathbf{r}_i)$, where $\theta_0(\mathbf{r}_i)$ is the value of the phase angle in the ground state and $\delta\theta(\mathbf{r}_i)$ is a smooth deviation, we can expand the Hamiltonian (1.3) for small $\delta\theta(\mathbf{r}_i)$,

$$\begin{aligned}\mathcal{H} &= -J \sum_{i\mu} \cos(\theta_0(\mathbf{r}_i + \hat{\mu}) - \theta_0(\mathbf{r}_i) - A_\mu(\mathbf{r}_i) + \delta\theta(\mathbf{r}_i + \hat{\mu}) - \delta\theta(\mathbf{r}_i)) \\ &\approx \frac{2NJ}{\sqrt{2}} + \frac{J}{2\sqrt{2}} \sum_{i\mu} (\delta\theta(\mathbf{r}_i + \hat{\mu}) - \delta\theta(\mathbf{r}_i))^2 \ , \end{aligned} \tag{1.9}$$

where we use $\cos(\theta_0(\mathbf{r}_i + \hat{\mu}) - \theta_0(\mathbf{r}_i) - A_\mu(\mathbf{r}_i)) = \cos(\pi/4) = 1/\sqrt{2}$ for all bonds in the ground state, and note that the linear term in $\delta\theta(\mathbf{r}_i)$ vanishes because we are expanding about the ground state. Assuming a smoothly varying $\delta\theta(\mathbf{r}_i)$, one can then compute the spin-spin correlation within this Gaussian spinwave approximation. The form of the Hamiltionian (1.9) is exactly the same as in the ordinary unfrustrated ($f = 0$) XY model, except for the factor $1/\sqrt{2}$. Proceeding with the

same steps as in the case of the ordinary XY model [12] one finds,

$$\langle \mathbf{S}(\mathbf{r}_i) \cdot \mathbf{S}(\mathbf{r}_j) \rangle = \mathrm{e}^{i(\theta_0(\mathbf{r}_j) - \theta_0(\mathbf{r}_i))} (\pi |\mathbf{r}_i - \mathbf{r}_j|)^{-\sqrt{2}T/2\pi J} \ , \tag{1.10}$$

where here, and throughout this chapter, we take $k_B = 1$.

Thus, within this spinwave approximation, spin correlations decay algebraically at all temperatures. Since the correlation vanishes as $r \to \infty$ there is no long-range phase angle ordering at low temperatures. Yet the algebraic decay, denoted *quasi-long-range order*, is still more ordered than the exponential decay one expects at sufficiently large temperatures. Thus the spinwave approximation must be leaving out essential excitations that convert the algebraic decay to exponential as temperature increases. These excitations are the fluctuation of vortices in the phase angles $\theta(\mathbf{r}_i)$ away from their ground state positions shown in Fig. 1.3.

A convenient measure of phase conherence in the system is given by the *helicity modulus*, $\Upsilon(T)$ [13, 14]. To define the helicity modulus, we need to consider the boundary conditions applied to a finite sample. We take our array to be a finite square of length $L$ in the $x$ and $y$ directions, with a total of $N = L^2$ sites. Rather than apply the usual periodic boundary conditions, we can apply *twisted boundary conditions*, requiring,

$$\theta(\mathbf{r}_i + L\hat{\mu}) = \theta(\mathbf{r}_i) + \Delta_\mu, \tag{1.11}$$

where $\Delta_\mu$ is the total phase angle twist applied across the system in direction $\hat{\mu} = \hat{x}, \hat{y}$.

We can now transform to a new set of variables,

$$\theta'(\mathbf{r}_i) \equiv \theta(\mathbf{r}_i) - \mathbf{r}_i \cdot \mathbf{\Delta}/L \tag{1.12}$$

so that the $\theta'(\mathbf{r}_i)$ obey periodic boundary conditions, $\theta'(\mathbf{r}_i + L\hat{\mu}) = \theta'(\mathbf{r}_i)$. The Hamiltonian then becomes,

$$\mathcal{H} = -J \sum_{i\mu} \cos(\theta'(\mathbf{r}_i + \hat{\mu}) - \theta'(\mathbf{r}_i) - A_\mu(\mathbf{r}_i) - \Delta_\mu/L) \ . \tag{1.13}$$

We can now ask if the free energy $\mathcal{F}$ of the system depends on the boundary twist $\mathbf{\Delta}$ that is applied. If $\mathcal{F}(\mathbf{\Delta})$ varies with $\mathbf{\Delta}$ then the system is sensitive to the boundary conditions; what happens at the boundary effects the bulk, hence the system has phase angle coherence. If $\mathcal{F}(\mathbf{\Delta})$ is independent of $\mathbf{\Delta}$, then what happens at the boundary has no effect on the bulk; the system has no phase angle ordering. In terms of the Josephson junction array analogy, a dependence of $\mathcal{F}(\mathbf{\Delta})$ on $\mathbf{\Delta}$ means that an applied phase angle twist drives a net supercurrent through the system; the array is superconducting with superconducting phase angle coherence. When $\mathcal{F}(\mathbf{\Delta})$ is independent of $\mathbf{\Delta}$, applying a phase angle twist causes no net supercurrent to flow; the array is in the normal state.

For the FFXY model, the ground state energy is a minimum when the twist $\mathbf{\Delta} = 0$. We can thus measure the dependence of $\mathcal{F}$ on $\mathbf{\Delta}$ by measuring the stiffness

of the free energy about this minimum. For small $\Delta_\mu$ we can approximate,

$$\mathcal{F}(\mathbf{\Delta}) \simeq \mathcal{F}(0) + \frac{1}{2}\Upsilon|\mathbf{\Delta}|^2 \ , \tag{1.14}$$

where the helicity modulus $\Upsilon$ is defined by,

$$\Upsilon_\mu \equiv \left.\frac{\partial^2 \mathcal{F}}{\partial \Delta_\mu^2}\right|_{\mathbf{\Delta}=0} \tag{1.15}$$

Using,

$$\mathcal{F}(\mathbf{\Delta}) = -T \ln Z(\mathbf{\Delta}) \tag{1.16}$$

with

$$Z(\mathbf{\Delta}) = \left(\prod_i \int_0^{2\pi} d\theta'(\mathbf{r}_i)\right) \exp(-\mathcal{H}[\theta'(\mathbf{r}_i);\mathbf{\Delta}]/T) \ , \tag{1.17}$$

we arrive at,

$$\begin{aligned}\Upsilon_\mu = &\frac{J}{N}\left\langle \sum_i \cos(\theta(\mathbf{r}_i+\hat{\mu}) - \theta(\mathbf{r}_i) - A_\mu(\mathbf{r}_i))\right\rangle \\ &- \frac{J^2}{TN}\left\langle \left[\sum_i \sin(\theta(\mathbf{r}_i+\hat{\mu}) - \theta(\mathbf{r}_i) - A_\mu(\mathbf{r}_i))\right]^2\right\rangle\end{aligned} \tag{1.18}$$

where the averages are evaluated in the untwisted ensemble $\mathbf{\Delta} = 0$. For the FFXY model one has $\Upsilon_x = \Upsilon_y$, hence we denote these simply as $\Upsilon$.

At low temperatures one can use the spinwave approximation to evaluate the helicity modulus. The calculation proceeds analogously to the case of the ordinary XY model [14], with the substitution $J \to J/\sqrt{2}$. To quadratic order in $\delta\theta(\mathbf{r}_i)$ only the first term in Eq. (1.18) contributes and one finds,

$$\Upsilon \approx \frac{J}{\sqrt{2}} - \frac{T}{4} \ . \tag{1.19}$$

Thus the spinwaves cause $\Upsilon$ to decrease as $T$ increases.

But the vanishing of the helicity modulus, marking the loss of quasi-long-range phase ordering, is due not to these spinwave fluctuations, but rather to vortex fluctuations, via the same mechanism proposed by Berezinskii [2] and by Kosterlitz and Thouless [3] for the ordinary XY model. We now sketch the Kosterlitz-Thouless argument for the instability of the system to vortex excitations.

Consider inserting a free (unpaired) vortex $n = +1$ superimposed on the ground state of the system. Summing phase angle differences going counterclockwise around any closed path containing the vortex yields, by definition, $2\pi$. Such a vortex would lead to a phase angle shift $\delta\theta(\mathbf{r}_i)$ at site $\mathbf{r}_i = (x, y)$, given by,

$$\delta\theta(\mathbf{r}_i) = \arctan\left[\frac{y - y_0}{x - x_0}\right] \tag{1.20}$$

where the vortex is located at position $\mathbf{r}_0 = (x_0, y_0)$ at the center of one of the cells of the array. Far from the center of the vortex, the phase angle shifts across any given bond are small, and so one can approximate $\delta\theta(\mathbf{r}_i + \hat{\mu}) - \delta\theta(\mathbf{r}_i) \approx \hat{\mu} \cdot \nabla\delta\theta(\mathbf{r}_i)$ and use the Hamiltonian of Eq. (1.9) to compute the total energy $E_v$ of adding the vortex. We get,

$$E_v \approx \frac{J}{2\sqrt{2}} \sum_{i\mu} |\hat{\mu} \cdot \nabla\delta\theta(\mathbf{r}_i)|^2 = \frac{J}{2\sqrt{2}} \sum_i \frac{1}{|\mathbf{r}_i - \mathbf{r}_0|^2} \tag{1.21}$$

$$\approx \frac{J}{2\sqrt{2}}\, 2\pi \int_1^R r dr \frac{1}{r^2} \approx \frac{\pi J}{\sqrt{2}} \ln R = \pi\Upsilon(0) \ln R \ , \tag{1.22}$$

where $R$ is the radial size of the array, and we used $\Upsilon(0) = J/\sqrt{2}$ for the zero temperature value of the helicity modulus. Note that the corrections to the result in Eq. (1.22) come from bonds close to the vortex center $\mathbf{r}_0$, where $\delta\theta(\mathbf{r}_i + \hat{\mu}) - \delta\theta(\mathbf{r}_i)$ is not necessarily small. However these corrections remain finite, and hence Eq. (1.22) gives the correct leading asymptotic behavior in the thermodynamic limit, $R \to \infty$.

At finite temperature, one should consider the *free energy* $F_v$ to add the vortex. This involves two important changes to Eq. (1.22). Firstly, one must consider the entropy $S$ associated with adding the vortex. In a system of radius $R$, there are $\pi R^2$ cells on which to center the vortex, and so $S = \ln \pi R^2$. Secondly, at finite $T$, one should replace $\Upsilon(0)$ in Eq. (1.22) by $\Upsilon(T)$, as can be argued as follows. The $\ln R$ term in Eq. (1.22) comes from putting a $2\pi$ phase angle twist around the vortex at large distances $r$ from the vortex center. This corresponds to a slowly varying phase angle gradient $1/r$. At $T \to 0$, when all thermal phase angle fluctuations are frozen out, the energy increase for inserting this phase angle twist is determined by the *bare spinwave stiffness* $J/\sqrt{2} = \Upsilon(0)$, as in the spinwave Hamiltonian (1.9). At finite $T$, however, the $2\pi$ twist around the vortex occurs in the presence of thermal fluctuations in the phase angles. One should thus replace the bare spinwave stiffness by a *renormalized spinwave stiffness* that measures the increase in free energy from applying slowly varying phase angle gradients in the presence of such thermal fluctuations. This is just the helicity modulus $\Upsilon(T)$. Thus the increase in free energy to add a vortex somewhere in the system is,

$$\begin{aligned} F_v &= \pi\Upsilon(T) \ln R - TS = \pi\Upsilon(T) \ln R - T \ln \pi R^2 \\ &\approx [\pi\Upsilon(T) - 2T] \ln R \ , \end{aligned} \tag{1.23}$$

to leading order as $R \to \infty$. For $\Upsilon(T) > 2T/\pi$, $F_v \to +\infty$ as $R \to \infty$. Adding a vortex then costs infinite free energy and so is suppressed. But for $\Upsilon(T) < 2T/\pi$, $F_v \to -\infty$ as $R \to \infty$, and such vortices are free to enter the sytem. Since $\Upsilon(T)$ is a monotonic decreasing function of $T$, we necessarily cross from the first case to the second as $T$ increases.

Once such a free vortex is thermally excited, it is free to diffuse throughout the system. Since the phase angle change going completely around a vortex must be $2\pi$, each time such a vortex moves a distance $\Delta y$ in the $\hat{y}$ direction, the net phase

angle twist across the system in the $\hat{x}$ direction changes by $2\pi\Delta y/L$ (assuming no other vortices have moved). Diffusion of free vortices can thus unwind any applied boundary twist $\mathbf{\Delta}$ and cause the system to lose all phase angle coherence, driving the helicity modulus $\Upsilon \to 0$. We thus have the famous Kosterlitz-Thouless stability criterion for a finite helicity modulus, and hence for phase angle coherence, which continues to hold for the fully frustrated model. If we denote $T_{\rm KT}$ as the Kosterlitz-Thouless temperature above which free vortices may be thermally excited and the system loses phase coherence, then

$$\Upsilon(T) \geq \frac{2}{\pi} T \qquad T \leq T_{\rm KT} \tag{1.24}$$

$$\Upsilon(T) = 0 \qquad T > T_{\rm TK} \tag{1.25}$$

We thus conclude that $\Upsilon(T)$ takes a discontinuous drop to zero as $T$ increases above $T_{\rm KT}$. If Eq. (1.24) holds as an equality at $T_{\rm KT}$, then $\Upsilon(T_{\rm KT})/T_{\rm KT} = 2/\pi$ has the same *universal jump* to zero found in the ordinary XY model [15, 16]. It is, however, possible that a first order transition or other mechanism could cause the loss of phase coherence to occur at a lower $T$, so that jump in $\Upsilon/T$ at the transition is larger than this universal value. The issue of whether this jump is the universal value or larger remains one of the often disputed questions concerning the FFXY model.

We return now to the spin-spin correlation function, considered previously in Eq. (1.10). The same argument concerning the replacement of the *bare* with the *renormalized* spin stiffness constant, that was used in going from Eq. (1.22) to (1.23), can be applied here to include the effects on the spin-spin correlation function of thermal excitations that go beyond the spinwave approximation. One thus replaces $\Upsilon(0) = J/\sqrt{2}$ in Eq. (1.10) by $\Upsilon(T)$ to arrive at,

$$\langle \mathbf{S}(\mathbf{r}_i) \cdot \mathbf{S}(\mathbf{r}_j) \rangle \sim |\mathbf{r}_i - \mathbf{r}_j|^{-\eta(T)} \quad , \quad \text{with} \quad \eta(T) = \frac{T}{2\pi\Upsilon(T)} \tag{1.26}$$

This result was first derived for the ordinary XY model by Berezinskii [2], and later by José et al. [17]. The condition of Eq. (1.24) then implies $\eta(T) \leq 1/4$, with $\eta(T_{\rm KT}) = 1/4$ if the universal jump in $\Upsilon/T$ holds. Above $T_{\rm KT}$, where $\Upsilon = 0$, Eq. (1.26) is consistent with the change in the spin-spin correlation from algebraic to exponential decay.

### 1.3.2. *Charge Lattice Ordering*

The ground state structure, shown in Fig. 1.3, consists of a checkerboard pattern of alternating "charges" $q_i \pm 1/2$ at sites in the centers of the square unit cells of the array. If we identify $q = +1/2$ with an up "spin" and $q = -1/2$ with a down "spin" ("spin" here having nothing to do with the real planar spins $\mathbf{S}(\mathbf{r}_i)$), then the ground state charge structure has the same symmetry as an antiferromagnetic Ising model. Accordingly, we can define a charge ordering parameter corresponding to

the "staggered magnetization",

$$M \equiv \sum_i (-1)^{x_i+y_i} q_i \tag{1.27}$$

where $q_i$ is the charge at the center of the cell located at position $\mathbf{r}_i = (x_i, y_i)$. The prefactor $(-1)^{x_i+y_i}$ thus alternates in sign on neighboring sites.

We expect that $\langle M \rangle$ is finite at sufficiently low temperatures, but that it vanishes above a well defined critical temperature $T_{\rm I}$. Since $\langle M \rangle$ is a scalar order parameter, we naively expect that this transition is in the Ising universality class, with critical exponents characteristic of the two dimensional Ising model. In this case, $\langle M \rangle$ should vanish continuously as $\langle M \rangle \sim (T_{\rm I} - T)^\beta$, with $\beta = 1/8$. Furthermore, we would expect there to be a logarithmically diverging specific heat ($\alpha = 0$) at $T_{\rm I}$ and a diverging correlation length $\xi_{\rm I} \sim |T - T_{\rm I}|^{-\nu}$ with $\nu = 1$. Whether or not the transition at $T_{\rm I}$ is indeed in the Ising universality class has been another of the main questions concerning the FFXY model.

### 1.3.3. *Summary*

To conclude this section we summarize the above main points. In the two dimensional FFXY model, we expect upon cooling to find a spontaneous breaking of the $U(1)$ symmetry at $T_{\rm KT}$ associated with the onset of phase angle coherence, and a breaking of the discrete $Z_2$ symmetry at $T_{\rm I}$ associated with the formation of an ordered charge lattice. The questions of interest are: (i) does $T_{\rm KT} = T_{\rm I}$, and if not, which is larger; (ii) is the phase angle ordering transition at $T_{\rm KT}$ in the universality class of the Berezinkii-Kosterlitz-Thouless transition of the ordinary 2D XY model; and (iii) is the charge lattice ordering transition at $T_{\rm I}$ in the Ising universality class?

## 1.4. Mapping to the Coulomb Gas

### 1.4.1. *Duality Transformation*

Considerable insight into the nature of the transitions in the 2D FFXY model can be obtained via a duality mapping onto an equivalent problem of two dimensional Coulomb interacting charges, as first shown by Kosterlitz and Thouless for the ordinary 2D XY model [3]. To simplify this duality transformation of the lattice FFXY model, it is customary to replace the cosine interaction of Eq. (1.3) with the Villain function [11] (sometimes referred to as the *periodic Gaussian* function) $V(\varphi)$, defined by,

$$\mathrm{e}^{-V(\varphi)/T} \equiv \sum_{m=-\infty}^{\infty} \mathrm{e}^{-J(\varphi+2\pi m)^2/2T} \tag{1.28}$$

The partition function, with twisted boundary conditions, then becomes,

$$Z(\mathbf{\Delta}) = \left( \prod_i \int_0^{2\pi} d\theta'(\mathbf{r}_i) \right) \left( \prod_{i\mu} \sum_{m_\mu(\mathbf{r}_i)=-\infty}^{\infty} \right) \mathrm{e}^{-\mathcal{H}[\theta'(\mathbf{r}_i), m_\mu(\mathbf{r}_i); \mathbf{\Delta}]/T} \tag{1.29}$$

where $m_\mu(\mathbf{r}_i)$ is an integer valued variable on each bond of the array and

$$\mathcal{H}[\theta'(\mathbf{r}_i), m_\mu(\mathbf{r}_i); \mathbf{\Delta}] = -\frac{J}{2} \sum_{i\mu} \left[ \theta'(\mathbf{r}_i + \hat{\mu}) - \theta'(\mathbf{r}_i) - A_\mu(\mathbf{r}_i) - \Delta_\mu/L + 2\pi m_\mu(\mathbf{r}_i) \right]^2 \tag{1.30}$$

We can think of the integers $m_\mu(\mathbf{r}_i)$ as representing the number of $2\pi$ twists in the phase angle $\theta$ as one crosses the bond from site $\mathbf{r}_i$ to site $\mathbf{r}_i + \hat{\mu}$.

Several different approaches to the duality transformation have been given in the literature [17–20]. Here we follow an approach due to Vallat and Beck [20], and derive the mapping for the case of the general uniformly frustrated XY model. We start by defining the "current" on each bond of the array as,

$$v_\mu(\mathbf{r}_i) \equiv \theta'(\mathbf{r}_i + \hat{\mu}) - \theta'(\mathbf{r}_i) - A_\mu(\mathbf{r}_i) - \Delta_\mu/L + 2\pi m_\mu(\mathbf{r}_i) \tag{1.31}$$

in terms of which

$$\mathcal{H} = \frac{J}{2} \sum_{i\mu} v_\mu^2(\mathbf{r}_i) \ . \tag{1.32}$$

Next we decompose $v_\mu(\mathbf{r}_i)$ into three pieces,

$$v_\mu(\mathbf{r}_i) = v_\mu^0 + v_\mu^T(\mathbf{r}_i) + v_\mu^L(\mathbf{r}_i) \tag{1.33}$$

where

$$v_\mu^0 \equiv \frac{1}{L^2} \sum_i v_\mu(\mathbf{r}_i) \tag{1.34}$$

is the average current flowing in the array in direction $\hat{\mu}$, and $v_\mu^T(\mathbf{r}_i)$ and $v_\mu^L(\mathbf{r}_i)$ are the transverse and longitudinal parts of $v_\mu(\mathbf{r}_i)$, defined by,

$$\mathbf{D} \cdot \mathbf{v}^T(\mathbf{r}_i) \equiv \sum_{\mu=x,y} [v_\mu^T(\mathbf{r}_i) - v_\mu^T(\mathbf{r}_i - \hat{\mu})] = 0 \tag{1.35}$$

$$\hat{z} \cdot [\mathbf{D} \times \mathbf{v}^L(\mathbf{r}_i)] \equiv v_x^L(\mathbf{r}_i) + v_y^L(\mathbf{r}_i + \hat{x}) - v_x^L(\mathbf{r}_i + \hat{y}) - v_y^L(\mathbf{r}_i) = 0 \tag{1.36}$$

where $\mathbf{D} \cdot \mathbf{v}$ is the discrete analog of divergence, and $\hat{z} \cdot [\mathbf{D} \times \mathbf{v}]$ is the discrete analog of the two dimensional curl, which is just the sum of the $v_\mu(\mathbf{r}_i)$ going counterclockwise around the unit cell of the array with lower left corner at $\mathbf{r}_i$. By definition, the spatial averages of $v_\mu^T(\mathbf{r}_i)$ and $v_\mu^L(\mathbf{r}_i)$ are zero.

Substituting the decomposition of Eq. (1.34) into the Hamiltonian (1.22), one can show that all the cross terms vanish and one gets,

$$\mathcal{H} = \frac{J}{2} \sum_{i\mu} \left\{ [v_\mu^0]^2 + [v_\mu^T(\mathbf{r}_i)]^2 + [v_\mu^L(\mathbf{r}_i)]^2 \right\} = \mathcal{H}^0 + \mathcal{H}^T + \mathcal{H}^L \ . \tag{1.37}$$

One can now solve for $v_\mu^T(\mathbf{r}_i)$ and $v_\mu^L(\mathbf{r}_i)$. The discrete difference operators behave just as do their continuum differential counterparts. Since the curl of $v_\mu^L(\mathbf{r}_i)$ vanishes, one can always write $v_\mu^L(\mathbf{r}_i)$ as the gradient of a scalar field $\chi(\mathbf{r}_i)$,

$$v_\mu^L(\mathbf{r}_i) = \chi(\mathbf{r}_i + \hat{\mu}) - \chi(\mathbf{r}_i) \ , \tag{1.38}$$

and since the spatial average of $v_\mu^L(\mathbf{r}_i)$ vanishes, the scalar field $\chi(\mathbf{r}_i)$ must satisfy periodic boundary conditions. The contribution of $v_\mu^L(\mathbf{r}_i)$ to the Hamiltonian is then just,

$$\mathcal{H}^L = \frac{J}{2} \sum_{i\mu} \left[ \chi(\mathbf{r}_i + \hat{\mu}) - \chi(\mathbf{r}_i) \right]^2 \ , \tag{1.39}$$

and has the same form as the spinwave approximation.

Since the divergence of $v_\mu^T(\mathbf{r}_i)$ vanishes, one can always write it in terms of a scalar field $\lambda(\mathbf{r}_i)$ such that

$$\mathbf{v}^T(\mathbf{r}_i) = \hat{z} \times \mathbf{D}\lambda(\mathbf{r}_i), \quad \text{with} \quad D_\mu \lambda(\mathbf{r}_i) \equiv \left[ \lambda(\mathbf{r}_i + \hat{\mu}) - \lambda(\mathbf{r}_i) \right] \ , \tag{1.40}$$

and since the spatial average of $v_\mu^T(\mathbf{r}_i)$ vanishes, the scalar field $\lambda(\mathbf{r}_i)$ must satisfy periodic boundary conditions. The contribution of $v_\mu^T(\mathbf{r}_i)$ to the Hamiltonian is then,

$$\mathcal{H}^T = \frac{J}{2} \sum_i |\hat{z} \times \mathbf{D}\lambda(\mathbf{r}_i)|^2 = \frac{J}{2} \sum_i |\mathbf{D}\lambda(\mathbf{r}_i)|^2 = -\frac{J}{2} \sum_i \lambda(\mathbf{r}_i) D^2 \lambda(\mathbf{r}_i) \tag{1.41}$$

where

$$D^2\lambda(\mathbf{r}_i) \equiv \sum_{\mu=x,y} \left[ \lambda(\mathbf{r}_i + \hat{\mu}) - 2\lambda(\mathbf{r}_i) + \lambda(\mathbf{r}_i - \hat{\mu}) \right] \tag{1.42}$$

is the discrete Laplacian operator, and we have "integrated" by parts in the last step of Eq. (1.41).

Unlike $\chi(\mathbf{r}_i)$, which make take any value, $\lambda(\mathbf{r}_i)$ is constrained as follows. The curl of $v_\mu^T(\mathbf{r}_i)$ must satisfy,

$$\hat{z} \cdot [\mathbf{D} \times \mathbf{v}^T(\mathbf{r}_i)] = \hat{z} \cdot [\mathbf{D} \times \mathbf{v}(\mathbf{r}_i)] = \hat{z} \cdot [\mathbf{D} \times 2\pi \mathbf{m}(\mathbf{r}_i)] - \hat{z} \cdot [\mathbf{D} \times \mathbf{A}(\mathbf{r}_i)] \tag{1.43}$$

as the contribution to the curl of $v_\mu(\mathbf{r}_i)$ from $[\theta'(\mathbf{r}_i + \hat{\mu}) - \theta'(\mathbf{r}_i)]$ and $\Delta_\mu / L$ vanishes. We then have,

$$\hat{z} \cdot [\mathbf{D} \times \mathbf{A}(\mathbf{r}_i)] \equiv 2\pi f \ , \tag{1.44}$$

with $f$ the uniform frustration arising from the circulation of the magnetic vector potential around the unit cell at $\mathbf{r}_i$, and we can define,

$$\hat{z} \cdot [\mathbf{D} \times 2\pi \mathbf{m}(\mathbf{r}_i)] \equiv 2\pi n(\mathbf{r}_i) \ , \tag{1.45}$$

with $n(\mathbf{r}_i)$ the integer vorticity at unit cell $i$, arising from the circulation of the phase angle twists $m_\mu(\mathbf{r}_i)$ around the cell.

We then have,

$$\hat{z} \cdot [\mathbf{D} \times \mathbf{v}^T(\mathbf{r}_i)] = 2\pi [n(\mathbf{r}_i) - f] \equiv 2\pi q(\mathbf{r}_i) \ , \tag{1.46}$$

with $q(\mathbf{r}_i)$ the "charge" centered on cell $i$.

We now write the curl of $v_\mu^T(\mathbf{r}_i)$ in terms of the scalar field $\lambda(\mathbf{r}_i)$,

$$\hat{z}\cdot[\mathbf{D}\times\mathbf{v}^T(\mathbf{r}_i)] = -\mathbf{D}\cdot[\hat{z}\times\mathbf{v}^T(\mathbf{r}_i)] = -\mathbf{D}\cdot[\hat{z}\times[\hat{z}\times\mathbf{D}\lambda(\mathbf{r}_i)]] = D^2\lambda(\mathbf{r}_i)\ , \quad (1.47)$$

which combined with Eq. (1.46) gives,

$$D^2\lambda(\mathbf{r}_i) = 2\pi q(\mathbf{r}_i)\ . \quad (1.48)$$

Hence $\lambda(\mathbf{r}_i)$ must solve the discrete Poisson equation with $q(\mathbf{r}_i)$ as the sources,

$$\lambda(\mathbf{r}_i) = -\sum_j G(\mathbf{r}_i-\mathbf{r}_j)q(\mathbf{r}_j) \quad (1.49)$$

where $G(\mathbf{r}_i-\mathbf{r}_j)$ is the lattice Green's function with periodic boundary conditions [17],

$$G(\mathbf{r}_i) = \frac{2\pi}{L^2}\sum_{\mathbf{k}}\frac{\mathrm{e}^{i\mathbf{q}\cdot\mathbf{r}_i}}{4-2\cos k_x-2\cos k_y}\ , \quad (1.50)$$

where one sums over all wavevectors $\mathbf{k}$ consistent with periodic boundary conditions, i.e. $k_\mu = 2\pi\ell_\mu/L$ with $\ell_\mu = 0,\dots L-1$. One has $G(\mathbf{r}) \sim -\ln|\mathbf{r}|$ for large $|\mathbf{r}|$. The contribution of $v_\mu^T(\mathbf{r}_i)$ to the Hamiltonian then becomes,

$$\mathcal{H}^T = -\frac{J}{2}\sum_i \lambda(\mathbf{r}_i)D^2\lambda(\mathbf{r}_i) = \pi J\sum_{i,j} q(\mathbf{r}_i)G(\mathbf{r}_i-\mathbf{r}_j)q(\mathbf{r}_j)\ , \quad (1.51)$$

which has precisely the form of a gas of charges $q(\mathbf{r}_i)$ interacting via the two dimensional Coulomb potential. Requiring $\mathcal{H}^T$ to be finite in the thermodynamic limit, $L\to\infty$, imposes the constraint of charge neutrality,

$$\sum_i q(\mathbf{r}_i) = 0\ , \quad \text{or} \quad \frac{1}{L^2}\sum_i n(\mathbf{r}_i) = f\ . \quad (1.52)$$

Finally we consider the spatial average $v_\mu^0$. Doing a discrete "integration" by parts, we have,

$$v_x^0 \equiv \frac{1}{L^2}\sum_{x=0}^{L-1}\sum_{y=0}^{L-1} v_x(x,y) = -\frac{1}{L^2}\sum_{x=0}^{L-1}\sum_{y=0}^{L-1} yD_y v_x(x,y) + \frac{1}{L}\sum_{x=0}^{L-1} v_x(x,0)\ , \quad (1.53)$$

where in the last term we made use of periodic boundary conditions $v_x(x,L) = v_x(x,0)$. The first term on the right hand side can be rewritten as,

$$-\frac{1}{L^2}\sum_{y=0}^{L-1} y\sum_{x=0}^{L-1} D_y v_x(x,y) = \frac{1}{L^2}\sum_y y\sum_x 2\pi q(x,y) = \frac{2\pi P_y}{L^2}\ , \quad (1.54)$$

where $P_y = \sum_i y_i q(\mathbf{r}_i)$ is the $y$ component of the total dipole moment in the system. The second term can be rewritten as,

$$\frac{1}{L}\sum_{x=0}^{L-1} v_x(x,0) = \frac{1}{L}(2\pi m_x^0 - \Delta_x)\ , \quad (1.55)$$

where we made use of the gauge choice of Eq. (1.6) to set $A_x(x,0)=0$, used periodic boundary conditions on $\theta'(\mathbf{r}_i)$ to conclude $\sum_x[\theta'(\mathbf{r}_i+\hat{x})-\theta'(\mathbf{r}_i)]=0$, and defined $m_x^0 \equiv \sum_x m_x(x,0)$ an integer.

Combining the above results gives,

$$v_x^0 = \frac{1}{L}\left(\frac{2\pi P_y}{L} - \Delta_x + 2\pi m_x^0\right) \quad . \tag{1.56}$$

A similar calculation gives,

$$v_y^0 = \frac{1}{L}\left(-\frac{2\pi P_x}{L} - \Delta_y + 2\pi m_y^0\right) \quad , \tag{1.57}$$

so that

$$\mathcal{H}^0 = \frac{J}{2}\left[\left(\frac{2\pi P_y}{L} - \Delta_x + 2\pi m_x^0\right)^2 + \left(-\frac{2\pi P_x}{L} - \Delta_y + 2\pi m_y^0\right)^2\right] \tag{1.58}$$

The above transformations have mapped the degrees of freedom from $\{\theta(\mathbf{r}_i), m_\mu(\mathbf{r}_i)\}$ to $\{\chi(\mathbf{r}_i), n(\mathbf{r}_i), m_x^0, m_y^0\}$. We can now evaluate the partition function summing over these new degrees of freedom. We group these sums as follows,

$$\begin{aligned} Z(\boldsymbol{\Delta}) = & \sum_{\{n(\mathbf{r}_i)\}} \mathrm{e}^{-\mathcal{H}^T[n(\mathbf{r}_i)]/T} \sum_{m_x^0, m_y^0=-\infty}^{\infty} \mathrm{e}^{-\mathcal{H}^0[n(\mathbf{r}_i), m_x^0, m_y^0]/T} \\ & \times \left(\prod_i \int_{-\infty}^{\infty} d\chi(\mathbf{r}_i)\right) \mathrm{e}^{-\mathcal{H}^L[\chi(\mathbf{r}_i)]/T} \end{aligned} \tag{1.59}$$

The Gaussian integrals in the last spinwave-like factor are easily done, and give an analytic multiplicative factor $Z_0(T)$ to the partition function. Since this term is independent of both the vortex degrees of freedom $n(\mathbf{r}_i)$ and the twist $\boldsymbol{\Delta}$, it plays no role in either the phase angle ordering or the vortex lattice ordering transition. In the XY model with Villain interaction, the spinwave excitations are thus completely decoupled from the vortex excitations, and we henceforth drop this term. Using Eq. (1.58) for $\mathcal{H}^0$, the sums over $m_x^0$ and $m_y^0$ can be done and they result in the Villain function $V(\varphi)$ of Eq. (1.28). We thus get the partition function of the dual Coulomb gas,

$$Z(\boldsymbol{\Delta}) = \sum_{\{n(\mathbf{r}_i)\}} \mathrm{e}^{-\mathcal{H}_{\mathrm{CG}}[n(\mathbf{r}_i)]/T} \tag{1.60}$$

where the sum over vortex configurations $\{n(\mathbf{r}_i)\}$ is constrained by the condition of charge neutrality, Eq. (1.52), and the Coulomb gas Hamiltonian is,

$$\mathcal{H}_{\mathrm{CG}} = V\left(\frac{2\pi P_y}{L} - \Delta_x\right) + V\left(-\frac{2\pi P_x}{L} - \Delta_y\right) + \pi J \sum_{i,j} q(\mathbf{r}_i) G(\mathbf{r}_i - \mathbf{r}_j) q(\mathbf{r}_j) \tag{1.61}$$

### 1.4.2. *Mechanisms for Destruction of Order*

Note, the terms in the Coulomb gas Hamiltonian involving the dipole moment $\mathbf{P}$ are the consequence of imposing the boundary condition with fixed twist $\mathbf{\Delta}$. In many derivations of the duality transformation, these terms were missing. Leaving off these terms corresponds to working in an ensemble in which the twist $\mathbf{\Delta}$ is free to fluctuate as a thermal degree of freedom. However, to get an expression for the helicity modulus in the dual Coulomb gas representation, it is important to keep them. From Eq. (1.15) we have,

$$\Upsilon_x = \left.\frac{\partial^2 \mathcal{F}}{\partial \Delta_x^2}\right|_{\mathbf{\Delta}=0} = \left\langle V''\left(\frac{2\pi P_y}{L}\right)\right\rangle - \frac{1}{T}\left\langle V'\left(\frac{2\pi P_y}{L}\right) V'\left(\frac{2\pi P_y}{L}\right)\right\rangle \ , \quad (1.62)$$

where $V'(\varphi)$ and $V''(\varphi)$ are the first and second derivatives of the Villain function. Note, at very low $T$ where the Villian function is approximately parabolic $V(\varphi) \approx \frac{1}{2}J\varphi^2$ for most of the interval $(-\pi, \pi]$, one has $V'' \approx J$ and $V'(\varphi) \approx J\varphi$, yielding,

$$\frac{\Upsilon_x}{J} \approx 1 - \frac{4\pi^2 J}{TL^2}\langle P_y^2\rangle \quad \text{at very low } T \ . \quad (1.63)$$

Eq. (1.63) was first dervied by Berezinskii [2] for the case of the ordinary XY model. Thus the helicity modulus is reduced by the fluctuations in the total dipole moment of the system, and the above leads to the identification $\Upsilon/J \equiv \epsilon^{-1}$, where $\epsilon$ is the dielectric function of the Coulomb gas.

The broken $U(1)$ and $Z_2$ symmetries of the low temperature ordered phase then suggest two different types of dipole excitations that cause $\Upsilon(T)$ to decrease from its $T = 0$ value as the system is heated. These are illustrated in Fig. 1.4. The excitation

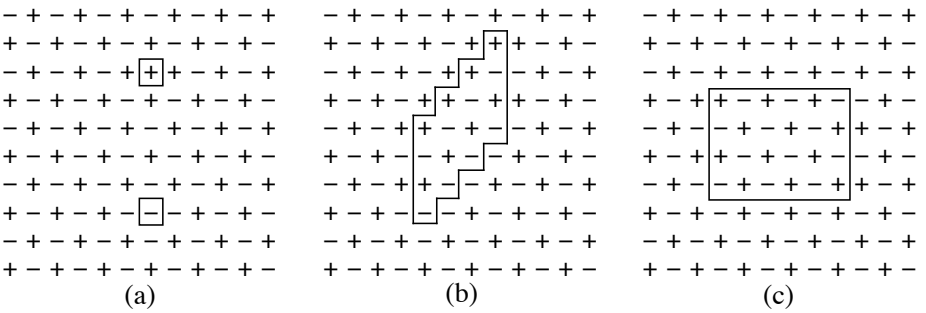


Fig. 1.4. Vortex excitations leading to a net dipole moment $P_y$. a) A vortex-antivortex pair excitation; b) An Ising-like domain excitation creating a net dipole moment; c) An Ising-like domain excitation with no net dipole moment. A (+) denotes a charge $q = +1/2$ while a (−) denotes a charge $-1/2$. Solid lines are bonds separating charges of equal sign.

in Fig. 1.4a is obtained by displacing one of the vortices $n = +1$ from its position $\mathbf{r}_i$ in the ground state, and moving it a distance $\mathbf{d}$ to a site $\mathbf{r}_j$ which previously had no vortex. The result is that $q(\mathbf{r}_i)$ changes from $+1/2$ to $-1/2$, while $q(\mathbf{r}_j)$ changes

from $-1/2$ to $1/2$, creating a net dipole moment $\mathbf{P} = \mathbf{d}$. Alternatively, we can view this excitation as the creation of a new vortex-antivortex pair with $n = +1$ at site $\mathbf{r}_j$ and $n = -1$ at site $\mathbf{r}_i$. The unbinding of such vortex-antivortex pairs, with $\mathbf{d}$ diffusing to large values, corresponds to the Kosterlitz-Thouless mechanism for the destruction of the $U(1)$ phase angle coherence at $T_{\rm KT}$ in the ordinary 2D XY model [3, 4].

The excitations in Figs. 1.4b and c are obtained by taking a closed domain of sites and flipping the sign of all the charges in the domain; to keep overall system charge neutrality, the domain itself must be charge neutral. Such flipped domains are Ising-like excitations and the growth of such domains leads to the vanishing of the $Z_2$ Ising-like order parameter $\langle M \rangle$ at $T_{\rm I}$. Depending on the precise shape of such domains, they may also create dipole moments as large as the area of the domain, as in the example shown in Fig. 1.4b, and thus also serve to decrease the helicity modulus $\Upsilon$.

It was further noticed by Halsey [21], that Ising-like excitations can be thought of as having fractional $\pm 1/4$ charges at the corners of the domain, as can be seen by coarse graining the charges over a $2 \times 2$ block of cells. The sum of these corner charges, going completely around the enclosing domain wall, must vanish for a neutral domain. It was suggested [21–24] that such corner charges played an important role: when the Ising-like transition occurs at $T_{\rm I}$, the domain wall tension will vanish, allowing paired $+1/4$ and $-1/4$ corner charges to unbind, thus destroying phase angle coherence by a similar pair unbinding mechanism as in Fig. 1.4a. Thus the Ising-like transition would necessarily trigger the KT-like transition. However, once the domain wall energy vanishes, domains of the type in Fig. 1.4b should also proliferate and become large, driving $\Upsilon \to 0$ through the large dipole moments created by such domains; domains with no net dipole moment, as in Fig 1.4c, could not lead to a reduction in $\Upsilon$ even if they became arbitrarily large with unbound corner charges, since the dipole moments of these corner charges must always sum to zero. Indeed, the coarse graining that gives rise to the corner charge picture is just an equivalent way to represent the net dipole moment that may appear on Ising-like domains. It is thus not clear that the transitions at $T_{\rm KT}$ or $T_{\rm I}$ are better understood in terms of a corner charge unbinding scenario. Nevertheless, we will see in a later section that a corner charge unbinding transition does indeed take place at a temperature well below $T_{\rm I}$, where the domain wall tension is still finite, and that this lower transition has crucial ramifications for the question as to whether $T_{\rm KT}$ is equal to, or less than, $T_{\rm I}$.

### 1.5. Numerical Results

The first numerical study of the 2D FFXY model was by Teitel and Jayaprakash [8] in 1983. Using ordinary Metropolis Monte Carlo simulations, they used Eq. (1.18) to compute the helicity modulus $\Upsilon(T)$, to investigate the vanishing of phase angle

coherence at $T_{\rm KT}$. They computed the specific heat $C$, using energy fluctuations, to look for the charge ordering transition at $T_{\rm I}$. If, as naively expected, the transition at $T_{\rm I}$ is in the universality class of the 2D Ising model, one expects a logarithmically diverging specific heat at $T_{\rm I}$. Their numerical results for $\Upsilon(T)$ and $C(T)$, for system sizes $L = 8 - 32$, are reprinted in Fig. 1.5. $\Upsilon$ appears to be taking a sharp drop to zero, that becomes steeper as $L$ increases, at a $T_{\rm KT}$ not inconsistent with the Kosterlitz-Thouless universal jump. The specific heat peak steadily increases with $L$, consistent with a $\ln L$ dependence, with the peak location approaching a $T_{\rm I}$ that is very close to $T_{\rm KT}$.

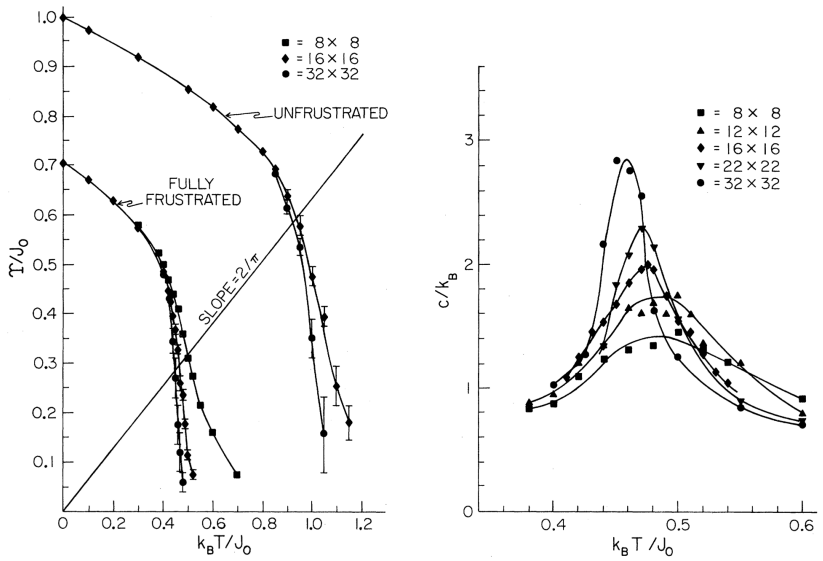


Fig. 1.5. Left: Helicity modulus $\Upsilon$ vs temperature $T$ for the unfrustrated ($f = 0$) and fully frustrated ($f = 1/2$) cases, and various lattice sizes $L \times L$. A line of slope $2/\pi$ indicates the universal jump in $\Upsilon(T_{\rm KT})/T_{\rm KT}$ of a Kosterlitz-Thouless transition. Right: Specific heat $C$ of the fully frustrated ($f = 1/2$) model for various lattice sizes $L \times L$. The smooth curves through the data are drawn as guides to the eye and are not the result of any theoretical computation. [Reprinted from Ref. [8]]

It is worthwhile to quote from Teitel and Jayaprakash's conclusions: "Two possible scenarios seem likely: (i) As $T_{\rm I}$ is approached from below, the Ising excitations [cf. Fig. 1.4b] result in a steep drop in $\Upsilon(T)$ from its low-$T$ value. As $\Upsilon/k_{\rm B}T$ approaches $2/\pi$, however, the KT excitations [cf. Fig. 1.4a] become important, producing a universal jump $2/\pi$ in $\Upsilon(T)/k_{\rm B}T$ at some temperature $T_{\rm KT} \leq T_{\rm I}$. (ii) As $T_{\rm I}$ is approached from below, the Ising excitations result in a nonuniversal jump in $\Upsilon/k_{\rm B}T > 2/\pi$ at the same temperature as the specific-heat peak $T_{\rm I}$. Our numerical simulations cannot adequately distinguish between these two possibilities."

In the following years, numerous theoretical and numerical works were carried out to try and resolve the three main questions: (1) is the jump in $\Upsilon/T$ at $T_{\rm KT}$ the universal $2/\pi$ or is it larger; (2) is the transition at $T_{\rm I}$ characterized by the critical exponents of the 2D Ising model; (3) is there only a single phase transition in the model with $T_{\rm KT} = T_{\rm I}$, or are there two separate transitions with $T_{\rm KT} < T_{\rm I}$? Theoretical analyses [24–30], based on symmetry arguments and renormalization group calculations, generally suggested a single phase transition $T_{\rm KT} = T_{\rm I}$ and nonuniversal jump in $\Upsilon$ at $T_{\rm KT}$. Numerical investigations were carried out on the original square lattice model of Eq. (1.3) [31–42], on the equivalent antiferromagnetic XY model on a triangular lattice (also fully frustrated) [32, 42–50], and on the dual lattice Coulomb gas model [51–54]. These numerical works generally led to conflicting conclusions on all of the above three questions.

Several extensions to the model were introduced in order to tune the separation between $T_{\rm KT}$ and $T_{\rm I}$ and so explore the fully frustrated model within the context of a larger parameter space. Berg et al. [55] introduced an asymmetric model in which the strength of the antiferromagnetic bond was set to $\eta J$, in comparison with the ferromagnetic bonds $-J$. Granato and Kosterlitz [30, 56] mapped this onto two coupled unfrustrated XY models with unequal couplings. Symmetry arguments [27, 28] led to a proposed coupled "XY-Ising" model believed to be in the same universality class as the FFXY model, and extensive theoretical and numerical analysis of this model was carried out by Granato, Kosterlitz, and coworkers [24, 57–59]. Thijssen and Knops [52, 53] introduced an additional term in the Coulomb gas model to tune the Ising-like domain wall energy. Cristofano *et al.* [60] related the FFXY model to behavior in more general twisted conformal field theories. Minnhagen and co-workers [61–63] modified the cosine interaction, $-J\cos(\varphi)$, to $(2J/p^2)[1-\cos^{2p^2}(\varphi/2)]$; $p = 1$ is the usual fully frustrated model, but for $p$ sufficiently large, the nature of the ground state changes. While these extended models led to interesting phase diagrams, in which $T_{\rm KT}$ and $T_{\rm I}$ could be clearly separated over large regions of the parameter space, numerical simulations at the specific point in the parameter space corresponding to the FFXY model generally lacked the accuracy to conclusively determine the behavior, and conflicting results remained.

The simplest and cleanest numerical demonstration that the FFXY model has two very close but distinct phase transitions, with $T_{\rm KT} < T_{\rm I}$, was given by Olsson [38] in 1996. Olsson utilized the Kosterlitz-Thouless stability criterion Eq. (1.24), $\Upsilon(T)/T \geq 2\pi$, to define the set of temperatures $T_L$ such that $\Upsilon(T_L, L)/T_L = 2\pi$, for finite systems with length up to $L = 128$. It was observed that the $T_L$ were monotonically decreasing with $L$, with a apparent finite limit as $L \to \infty$, thus providing an upper bound on $T_{\rm KT}$. Olsson then measured the staggered magnetization at these points, $M_L \equiv \langle M(T_L, L)\rangle$, and observed that the $M_L$ monotonically *increased* with increasing $L$, thus demonstrating that $M(T_{\rm KT}) \geq \lim_{L\to\infty} M_L$ must be finite as $L \to \infty$. In Fig. 1.6 we show Olsson's results from Ref. [38], plotting

$\langle M \rangle$ vs $\Upsilon\pi/(2T)$ for various system sizes $L$. The dashed vertical line defines the temperatures $T_L$.

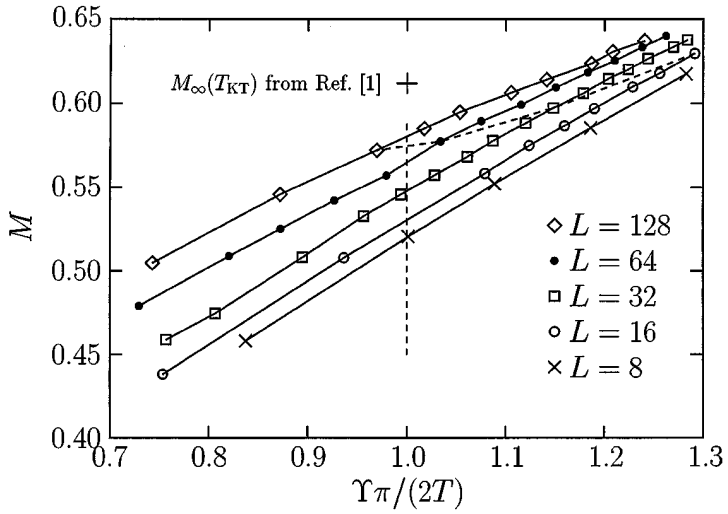


Fig. 1.6. Plot of staggered magnetization $\langle M \rangle$ vs $\Upsilon\pi/(2T)$ for systems of different length $L$, for the FFXY model with cosine interaction on a square lattice. For $L = 64$ and 128 the temperature difference between the neighboring points is $0.001J$. The vertical dashed line determines $T_L$, the size dependent upper bound on $T_{\rm KT}$, as obtained via the Kosterlitz-Thouless stability condition, $\Upsilon(T_{\rm KT}) \geq (2\pi)/T_{\rm KT}$. That $M_L \equiv \langle M(T_L, L) \rangle$ increases monotonically with increasing $L$ along this dashed vertical line indicates that $M(T_{\rm KT})$ is finite in the thermodynamic limit, and hence $T_{\rm KT} < T_{\rm I}$. [Reprinted from Ref. [38]]

For two separated transitions, $T_{\rm KT} < T_{\rm I}$, the general expectation has been that the loss of $Z_2$ symmetry at the transition $T_{\rm I}$ should be in the usual 2D Ising universality class, while the loss of $U(1)$ symmetry at $T_{\rm KT}$ should be in the Kosterlitz-Thouless universality class, with a universal jump in the helicity modulus, $\Upsilon(T_{\rm KT})/T_{\rm KT} = 2\pi$. Olsson [37–39] has provided numerical support for this scenario and noted that the non-Ising critical exponents at $T_{\rm I}$ often cited in the literature are most likely due to crossover effects resulting from the very close proximity of $T_{\rm KT}$ to $T_{\rm I}$ (see also Ref. [62] for a related point of view). This scenario has been confirmed in very recent high precision numerical simulations by Hasenbusch *et al.* [64, 65], who carried out detailed finite size scaling analyses using the largest system sizes to date, $L = 1000$. Among their findings is that the spin correlation length $\xi_s$, obtained from the exponential decay of the spin-spin correlation function Eq. (1.10) above $T_{\rm KT}$, is $\xi_s \simeq 120$ at $T = T_{\rm I}$, thus confirming that the non-Ising exponents reported in earlier works are due to crossover effects dominating the results for too small system sizes $L$. A nice, detailed, review of earlier numerical results is presented by these authors in Ref. [65]. The most recent numerical simulations of

the FFXY model by Okumura *et al.* [66], also using system sizes up to $L = 1000$, confirm the results of Hasenbusch *et al.* that there are two close but distinct transitions $T_{\rm KT} < T_{\rm I}$, that the transition at $T_{\rm I}$ is characterized by the usual 2D Ising critical exponents, and that $\xi_s(T_{\rm I}) \simeq 120$. However their analysis finds a slightly lower value of $T_{\rm KT}$ and that, while the phase angle disordering transition is still continuous, the jump in $\Upsilon(T_{\rm KT})/T_{\rm KT}$ is larger than the expected universal value $2/\pi$.

### 1.6. Kink-Antikink Unbinding Transition

While Olsson [38] convincingly demonstrated in 1996 that the FFXY model did indeed have two distinct transitions $T_{\rm KT} < T_{\rm I}$, it remained until 2002 for Korshunov [67] to provide the theoretical understanding behind this phenomenon, in terms of the unbinding of kink-antikink pairs that occur along the domain walls of Ising-like excitations, such as shown in Figs. 1.4b and 1.4c.

Korshunov's argument can be rephrased in terms of the dual Coulomb gas model introduced in section 1.4. As $T$ increases to $T_{\rm I}$, increasingly large Ising-like domains get excited in the system. If such domains can carry a net dipole moment that scales with the size of the domain $\xi_{\rm I}$, such as in Fig. 1.4b, and if $\xi_{\rm I}$ diverges continuously upon approaching $T_{\rm I}$, $\xi_{\rm I} \sim |T - T_{\rm I}|^{-\nu}$, then by Eqs. (1.62-1.63) diverging dipole fluctuations would drive the inverse dielectric constant $\epsilon^{-1}$, and hence the helicity modulus $\Upsilon \equiv J\epsilon^{-1}$, *continuously* to zero at $T_{\rm I}$. However the Kosterlitz-Thouless stability criterion of Eq. (1.24) ensures that $\Upsilon$ may not go continuously to zero; once $\Upsilon/T$ falls below $2/\pi$, vortex-antivortex pair excitations as in Fig. 1.4a unbind to produce freely diffusing vortices that drive $\Upsilon$ discontinuously to zero. This necessarily happens at a $T_{\rm KT}$ that must be lower than $T_{\rm I}$, unless a first order phase transition preempts the continuous Ising-like transition and drives both $\Upsilon$ and $\langle M \rangle$ discontinously to zero at a common temperature.

However, for a domain excitation to be considered "Ising-like", the free energy to create the domain should scale proportional to the domain wall length. Because the charges in the Coulomb gas interact with a long range logarithmic potential, one finds that at $T = 0$, and presumably also at sufficiently low $T$, the only domains for which the excitation energy scales proportional to wall length are those which have *zero* total dipole moment! Such domains, as in Fig. 1.4c, cannot contribute to any reduction in $\Upsilon$. If this remained true up to high temperatures, it would suggest that the loss of Ising-like order with the vanishing of $\langle M \rangle$ might be completely decoupled from the loss of phase angle coherence with the vanishing of $\Upsilon$. Korshunov demonstrated, however, that this does not remain true due to an unbinding of kink-antikink pairs along the domain wall, that takes place at a $T_{\rm w}$ well below $T_{\rm I}$.

We are interested in the behavior of domains that become large on the scale of the system length $L$. Let us therefore imagine a system containing a single domain

wall running the length of the system. One can introduce such a domain wall by choosing a system of size $L\times(L+1)$, with $L$ even. The $2\times2$ repeated cell structure of the ground state, as shown in Fig. 1.3, then ensures that the ground state necessarily contains such a system spanning domain wall. The lowest energy configuration for such a domain wall would be perfectly flat, as illustrated in Fig. 1.7a. The simplest excitation of the domain wall would consist of a single *kink* of unit step height, as illustrated in Fig. 1.7b. However, as discussed at the end of section 1.4.2, each corner of a domain wall can be thought of as consisting of a net localized charge of $q = \pm1/4$. As the two corner charges of a kink have the same sign, the net charge of a kink is $q_{\rm kink} = \pm1/2$ (for the kink of Fig. 1.7b, $q_{\rm kink} = +1/2$). An isolated kink, as in Fig. 1.7b, would therefore destroy charge neutrality and have a Coulomb energy that grows proportional to $\ln L$.

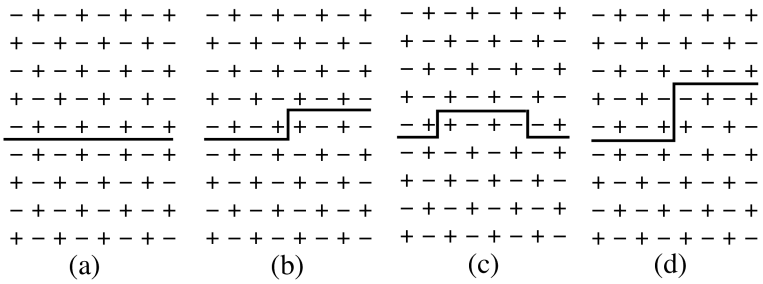


Fig. 1.7. Various configurations of the domain wall in a $L\times(L+1)$ system: (a) ground state, (b) isolated kink of unit height, (b) finite width step of unit height (kink-antikink pair), (d) isolated kink of height two. A (+) indicates the presence of a vortex in the XY model, or a charge $q_i = +1/2$ in the dual Coulomb gas; a (−) indicates the absence of a vortex, or a charge $q_i = -1/2$.

To keep the excitation energy finite, such kinks must therefore appear only as *kink-antikink pairs*, separated by a length $\ell$, where $\ell$ must be even to preserve charge neutrality. The energy of the pair is then finite and proportional to $\ln\ell$. Such a kink-antikink pair, as illustrated in Fig. 1.7c, creates a net dipole moment in the system, $p_x = q_{\rm kink}\ell$. At low temperatures, the $\ln\ell$ energy keeps kink-antikink pairs confined to small separations $\ell \le \ell^*(T)$. However, as $T$ increases, the entropy associated with the placement of the kinks will cause a reduction in the free energy of such excitations, leading to a *kink-antinkink unbinding transition* at a $T_{\rm w}$ where $\ell^*(T_{\rm w}) \to \infty$. Above $T_{\rm w}$, large dipole moments can thus form on the Ising-like domains with no increase in free energy, except for a contribution that is proportional to the length of the domain wall. If $T_{\rm w} < T_{\rm I}$, we then recover the argument for $T_{\rm KT} < T_{\rm I}$ outlined at the start of this section.

So far we have discussed only kinks of unit height. One may also have kinks of general height $h$. A kink of $h = 2$ is illustrated in Fig. 1.7d. For $h$ odd, the two corner charges that comprise the kink have the same sign, and so such kinks

must again be paired with antikink(s) of equal opposite total charge. For $h$ even, however, the two corner charges of the kink have the *opposite* sign, and the energy of an isolated kink is therefore finite and proportional to $\ln h$. Such kinks may thus be excited at any finite temperature. Note, however, that kinks with even $h$ do not create any net dipole moment in the system. Such even-step kinks can thus act to roughen domain walls, however they cannot contribute to a reduction in $\Upsilon$.

The preceding discussion can also be cast in terms of the phase angle coherence in the system, as originally presented by Korshunov. When a unit-step kink-antikink pair unbinds, and the domain wall of Fig. 1.7a shifts by one lattice spacing, the net phase angle twist $\Delta_y$ across the system changes by $\pi$ (a shift in the wall by two lattice spacing induces a twist of $2\pi$, which is equivalent to zero). Above $T_{\rm w}$, such domain wall fluctuations therefore lead to fluctuating phase shifts between opposite sides of the domain wall, leading to the destruction of phase coherence across the domain wall. As $T_{\rm I}$ is approached from below, and the size of the largest thermally excited domain diverges continuously, phase coherence across the system would vanish continuously. As $\Upsilon(T)$ decreases due to the domain excitations, the Kosterlitz-Thouless vortex instability is triggered at a $T_{\rm KT} < T_{\rm I}$, causing $\Upsilon$ to drop discontinuously to zero and destroying phase coherence.

We conclude by presenting the Kosterlitz-Thouless-like argument for the kink-antikink unbinding transition [68]. From Eq. (1.61), the energy of an isolated unit-step kink along a system spanning domain wall of length $L$ is,

$$E_{\rm kink} = \pi \Upsilon q_{\rm kink}^2 G(L) \approx \frac{\pi}{4} \Upsilon \ln L \tag{1.64}$$

In the above expression, we have replaced the bare coupling constant $J$ of Eq. (1.61) with $\Upsilon = J\epsilon^{-1}$, so as to allow for the screening effects of other charge excitations elsewhere in the system. The entropy associated with the position of the kink along the domain wall is,

$$S_{\rm kink} = \ln L \tag{1.65}$$

The free energy for the isolated unit-step kink is therefore,

$$F_{\rm kink} = E_{\rm kink} - T S_{\rm kink} = \left[ \frac{\pi}{4} \Upsilon - T \right] \ln L \tag{1.66}$$

The domain was thus becomes unstable to the appearance of free unit-step kinks (due to the unbinding of kink-antikink pairs) when,

$$T_{\rm w} = \frac{\pi}{4} \Upsilon(T_{\rm w}) \ . \tag{1.67}$$

Comparing to the similar criterion Eq. (1.23) for the instability of the system to the appearance of free vortices (due to the unbinding of vortex-antivortex pairs),

$$T_{\rm KT} = \frac{\pi}{2} \Upsilon(T_{\rm KT}) \ , \tag{1.68}$$

we can thus, ignoring the temperature dependence of $\Upsilon$, estimate,

$$T_{\rm w} \approx \frac{1}{2} T_{\rm KT} \ . \tag{1.69}$$

Thus, as desired, the kink-antikink unbinding transition takes place well below the bulk transitions of the system. Numerical evidence for this kink-antikink unbinding scenario was given by Olsson and Teitel in Ref. [69].

### 1.7. FFXY on a Honeycomb Lattice

In the fully frustrated XY model on a triangular lattice, the charges of the dual Coulomb gas sit on the sites of a honeycomb lattice, and have a ground state structure as shown in Fig. 1.8. The ground state is thus doubly degenerate and breaks the same $Z_2$ symmetry as does the FFXY on a square lattice. As discussed above, we therefore expect the transitions of the FFXY on the triangular lattice to be qualitatively the same as those on the square lattice. However a FFXY on a honeycomb lattice, in which the charges $q_i = \pm 1/2$ sit on the sites of the dual triangular lattice, is a more complex problem with a higher degeneracy of ground states. This case was first numerically simulated in the XY formulation by Shih and Stroud [46], then discussed theoretically by Korshunov [23]. Numerical study of the dual Coulomb gas on a triangular lattice was carried out by Lee and Teitel [70].

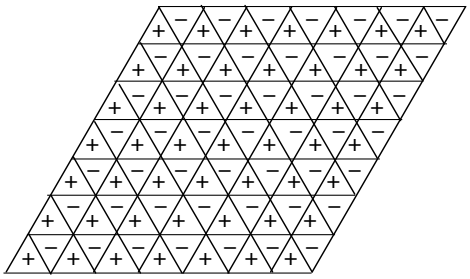

Fig. 1.8. Configuration of charges $q_i = \pm 1/2$ in the ground state of the FFXY on a triangular lattice. The ground state has a double discrete degeneracy just as is the case for the FFXY on a square lattice.

Since charges of the same sign repel each other, the ground state configuration would like to have charges of opposite sign in nearest neighbor cells. For square or triangular lattices, a state is easily constructed which satisfies this condition simultaneously for each pair of neighboring cells, as in Figs. 1.3 and 1.8. However, for the XY honeycomb lattice, the geometry frustrates the construction of any such state; no matter how one tries to put down equal numbers of $+1/2$ and $-1/2$ charges, one inevitably must wind up with neighboring cells which are occupied by charges of the same sign. This leads to a high degeneracy of ground states.

Recall, the ordinary short range antiferromagnetic Ising model on a triangular lattice is fully frustrated and has a ground state degeneracy that grows exponentially with the number of sites $N$, and thus has a finite $T = 0$ entropy density. In the

$f = 1/2$ Coulomb gas on the triangular lattice, dual to the FFXY on the honeycomb lattice, the long range logarithmic interactions lift much of the degeneracy found in the corresponding Ising model, and the degeneracy of the ground state is $3(2^L)$, for a system of length $L$, thus giving a vanishing ground state entropy density [70]. A sample ground state is shown in Fig. 1.9a.

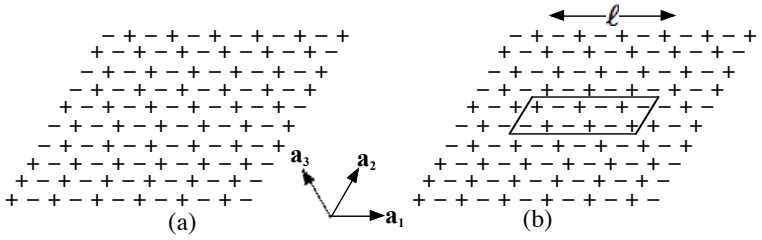


Fig. 1.9. (a) An example of a ground state of the $f = 1/2$ Coulomb Gas on a triangular lattice, which is dual to the FFXY model on a honeycomb lattice. A (+) is a charge $q_i = +1/2$, while a (−) is a charge $q_i = -1/2$. In a given direction, here $\mathbf{a}_1$, charges in each row alternate in sign, while in alternative directions the charges are sequenced randomly. The three lattice directions $\mathbf{a}_1$, $\mathbf{a}_2$ and $\mathbf{a}_3$ are indicated. (b) An example of a $2 \times \ell$ domain excitation that, as $\ell \to \infty$, leads to transitions among the different grounds states with the same ordering direction.

The ground states may be described as follows. Pick one of the three directions $\mathbf{a}_i$ that define the triangular lattice. In each row oriented in this direction, the charges alternate in sign; we will refer to this as the *ordering direction*. In either of the two other directions $\mathbf{a}_j$, $j \neq i$ (which we will call the *complementary directions*), the charges may be sequenced completely at random. The reason for this degeneracy is easily seen in the dual Coulomb gas, where the Coulomb interaction on the triangular lattice is given by [71],

$$G(\mathbf{r}) = \frac{\sqrt{3}\pi}{N} \sum_{\mathbf{k}} \mathrm{e}^{i\mathbf{k}\cdot\mathbf{r}} G_{\mathbf{k}}, \quad G_{\mathbf{k}} \equiv \frac{1}{3 - \cos(\mathbf{k}\cdot\mathbf{a}_1) - \cos(\mathbf{k}\cdot\mathbf{a}_2) - \cos(\mathbf{k}\cdot\mathbf{a}_3)}. \tag{1.70}$$

If the charges alternate in sign along the direction $\mathbf{a}_1$, as for example in Fig. 1.9a, then the only wavevectors $\mathbf{k}$ that appear in the Fourier transform of the charge distribution $q(\mathbf{r}_i)$ must satisfty $\mathbf{k}\cdot\mathbf{a}_1 = \pi$. Since $\mathbf{a}_3 = \mathbf{a}_2 - \mathbf{a}_1$, we then get $\cos(\mathbf{k}\cdot\mathbf{a}_3) = \cos(\mathbf{k}\cdot[\mathbf{a}_2 - \mathbf{a}_1]) = \cos(\mathbf{k}\cdot\mathbf{a}_2 - \pi) = -\cos(\mathbf{k}\cdot\mathbf{a}_2)$, and hence $G_{\mathbf{k}}$ is independent of the component of $\mathbf{k}$ perpendicular to $\mathbf{a}_1$. Since the Coulomb interaction part of the energy can be written in terms of Fourier transforms as $\propto \sum_{\mathbf{k}} q_{\mathbf{k}} G_{\mathbf{k}} q_{-\mathbf{k}}$, the energy of such a configuration is independent of the sequence of charges in the complementary directions.

Korshunov [23] has noted that this degeneracy holds for any $2\pi$-periodic interaction potential $V(\varphi)$. For the specific case of the Villain interaction of Eq. 1.28, in which spinwave excitations completely decouple from the vortex excitations (see

section 1.4.1), Lee and Teitel [70] have shown that domain excitations of size $2 \times \ell$, such as shown in Fig. 1.9b, have an energy that saturates to a finite value as $\ell \to \infty$. Thus the free energy barrier for transitions between the different possible random sequences for a given ordering direction $\mathbf{a}_i$ remains finite, and transitions may occur at any finite $T$. Whether the system has a sharp transition at a finite temperature into the *class* of states specified by a given ordering direction remains an open question. Similarly, since the excitations illustrated in Fig. 1.8b create no net dipole moment, it is still an open question whether there exists a finite temperature phase angle ordering transition below which $\Upsilon$ is finite.

Korshunov [23] proposed that for interactions other than Villain's, such as the physical one for Josephson junctions $V(\varphi) = -J\cos\varphi$, in which spinwave-vortex interactions are present [14], thermal fluctuations will give contributions to the free energy that may lift the degeneracy among the ground states at finite low temperatures. In a recent work Korshunov and Douçot [72] have shown that such a fluctuation effect indeed occurs, but only at the anharmonic order. In this case, domain walls as in Fig. 1.9b acquire a finite free energy per unit length, $F_{\rm d}/\ell \sim \gamma T^2/J$, with $\gamma \sim 10^{-4}$, and the free energy of different ground states is similarly shifted by an amount $\sim \gamma T^2/J$ per unit cell; the lowest energy state is one in which the charges all have the same sign when looking in one of the complimentary directions. The smallness of the coefficient $\gamma$, however, implies that one needs to have very large lattice sizes (Korshunov estimates $L > 10^5$), in order for the total free energy of a system spanning domain wall to be greater than the proposed critical temperature of an ordering transition, and hence to observe the fluctuation induced ordering. Very similar effects have been reported by Korshunov [73, 74] for the FFXY on a dice lattice (with dual Coulomb gas on a kagome lattice).

## 1.8. Conclusions

In this chapter we have endeavored to describe the rich phenomena associated with the fully frustrated XY model on different lattices. Many of the key concepts in understanding this phenomena have their clear origin in the ideas of Berezinskii and of Kosterlitz and Thouless. The broader class of uniformly frustrated XY models offers an even richer set of systems in which to explore the relation between continuous and discrete symmetries, and complex spatial ground states. Numerous works have explored specific cases. Denniston and Tang [75, 76] have shown that for the $f = 1/3$ model on a square lattice, and the $f = 2/5$ on a square lattice with quenched bond disorder, the vortex pattern ordering transition is in the same universality class as the ordinary 2D Ising model, whereas the pure $f = 2/5$ model has a first-order transition. Kolahchi and Straley have shown that for $f = 5/11$ on a square lattice, the ground state consists of a periodic superlattice of vacancies on the otherwise checkerboard pattern of $f = 1/2$, with the basic periodic cell of that structure having size $22 \times 22$ in contrast to earlier suggestions [9] that for $f = p/q$

the ground state would always be compatible with a $q \times q$ periodic cell. Franz and Teitel [78] found for this $f = 5/11$ case that, upon heating, the superlattice of vacancies first melted to a liquid while preserving the background checkerboard $f = 1/2$-like structure, and only at a higher temperature did the $f = 1/2$-like structure itself melt. Franz and Teitel [78], and later Gotcheva and Teitel [79] studied dilute frustrations $f = 1/q$ on triangular and square lattices, finding, for $q$ large enough, distinct vortex lattice unpinning and vortex lattice melting transitions upon heating the ground state. Korshunov *et al.* [80], have studied the cases $f = 1/4$ and $f = 1/3$ on a triangular lattice, and found large ground state degeneracies similar to those discussed above for $f = 1/2$ on the honeycomb lattice.

Considerable effort has gone into attempts to understand the behavior at *irrational* values of the frustration, in particular the frustration $f^* = (3-\sqrt{5})/2$, which is related to the golden mean. In the first study of this model, Halsey [81] proposed that the system had a finite temperature transition into a disordered but frozen vortex glass state. However subsequent study of the Coulomb gas version of the model by Gupta *et al.* [82], and of the XY version of the model by Denniston and Tang [83] and by Kolahchi and Fazli [84], found evidence for a finite temperature transition $T_c$ to an ordered vortex pattern. Although it appears that the ground states of the system at $f^*$ may depend in detail upon the precise form of the interaction potential $V(\varphi)$, for both the Villain interaction (i.e. the Coulomb gas model) and the cosine interaction, the ordered vortex structure below $T_c$ appears to possess anisotropic phase angle coherence, with the helicity modulus becoming finite in one direction, while remaining zero in the orthogonal direction until a much lower temperature where all vortices become pinned. Other recent works [85–87], however, have argued for a zero temperature glass transition.

Determining the ground state vortex pattern for a general $f = p/q$ has received considerable attention. Straley and Barnett [88] determined ground states for all cases with $q \leq 20$ for the cosine XY model, and found that the periodicity of the ground state can in general be larger than $q$. Denniston and Tang [83] have found that ground state periodicity may be as large as $q^2$. Kolahchi [89, 90] has proposed schemes to generate potential ground states for rational and irrational frustrations of the cosine XY model. Lee *et al.* [91] have proposed a scheme to construct ground states for all $1/3 < f < 1/2$ in the dual Coulomb gas. A comprehensive review of the many facets of the general uniformly frustrated XY model lies outside the scope of this short chapter. We therefore conclude with the observation that much rich phenomena remains to be explored.

## Acknowlegments

I am grateful to the many colleagues from whom I learned about the XY model, and the many colleagues and students who joined me in working on related problems. These include, Vinay Ambegaokar, Petter Minnhagen, C. Jayaprakash, David

Stroud, Eytan Domany, K. K. Mon, Ying-hong Li, Jong-Rim Lee, John Chiu, Peter Olsson, Marcel Franz, Michel Gingras, Pramod Gupta, Tao Chen, and Violeta Gotcheva.

## References

[1] V. L. Berezinskii, Violation of Long Range Order in One-Dimensional and Two-Dimensional Systems with a Continuous Symmetry Group. I. Classical Systems, *Zh. Eksp. Teor. Fiz.* **59**, 907 (1970); [*Sov. Phys.–JETP* **32**, 493 (1971)].

[2] V. L. Berezinskii, Violation of Long Range Order in One-Dimensional and Two-Dimensional Systems with a Continuous Symmetry Group. II. Quantum Systems, *Zh. Eksp. Teor. Fiz.* **61**, 1144 (1971); [*Sov. Phys.–JETP* **34**, 610 (1972)].

[3] J. M. Kosterlitz and D. J. Thouless, Ordering, Metastability and Phase Transitions in Two-Dimensional Systems, *J. Phys. C* **6**, 1181 (1973).

[4] J. M. Kosterlitz, The Critical Properties of the Two-Dimensional XY Model, *J. Phys. C* **7**, 1046 (1974).

[5] D. J. Resnick, J. C. Garland, J. T. Boyd, S. Shoemaker and R. S. Newrock, Kosterlitz-Thouless Transition in Proximity-Coupled Superconducting Arrays, *Phys. Rev. Lett.* **47**, 1542 (1981).

[6] R. F. Voss and R. W. Webb, Phase Coherence in a Weekly Coupled Array of 20 000 NB Josephson Junctions, *Phys. Rev. B* **25**, 3446 (1982).

[7] C. J. Lobb, Josephson Junction Arrays and Superconducting Wire Networks, *Hel. Phys. Acta* **65**, 219 (1992).

[8] S. Teitel and C. Jayaprakash, Phase Transitions in Frustrated Two-Dimensional XY Models, *Phys. Rev. B* **27**, 598 (1983).

[9] S. Teitel and C. Jayaprakash, Josephson-Junction Arrays in Transverse Magnetic Fields, *Phys. Rev. Lett.* **51**, 1999 (1983).

[10] J. Villain, Spin Glass with Non-Random Interactions, *J. Phys. C* **10**, 1717 (1977).

[11] J. Villain, Two-Level Systems in a Spin-Glas Model: I. General Formalism and Two-Dimensional Model, *J. Phys. C* **10**, 4793 (1977).

[12] See, for example, M. Plischke and B. Bergersen, *Equilibrium Statistical Physics, 3rd ed.* (World Scientific, Singapore, 2006), section 6.6.

[13] M. E. Fisher, M. N. Barber and D. Jasnow, Helicity Modulus, Superfluidity, and Scaling in Isotropic Systems, *Phys. Rev. A* **8** 1111 (1973).

[14] T. Ohta and D. Jasnow, XY Model and the Superfluid Density in Two Dimensions, *Phys. Rev. B* **20**, 139 (1979).

[15] D. R. Nelson and J. M. Kosterlitz, Universal Jump in the Superfluid Density of Two-Dimensional Superfluids, *Phys. Rev. Lett.* **39**, 1201 (1977).

[16] P. Minnhagen and G. G. Warren, Superfluid Density of a Two-Dimensional Fluid, *Phys. Rev. B* **24**, 2526 (1981).

[17] J. José, L. P. Kadanoff, S. Kirkpatrick and D. R. Nelson, Renormalization, Vortices, and Symmetry-Breaking Perturbations in the Two-Dimensional Planar Model, *Phys. Rev. B* **16** 1217 (1977).

[18] E. Fradkin, B. Huberman and S. H. Shenker, Gauge Symmetries in Random Magnetic Systems, *Phys. Rev. B* **18**, 4789 (1978).

[19] R. Savit, Vortices and the Low-Temperature Structure of the X-Y Model, *Phys. Rev. B* **17**, 1340 (1978).

[20] A. Vallat and H. Beck, Coulomb-Gas Representation of the Two-Dimensional XY Model on a Torus, *Phys. Rev. B* **50**, 4015 (1994).

[21] T. C. Halsey, Topological Defects in the Fully Frustrated XY Model and in $^3$He-A Films, *J. Phys. C* 18, 2437 (1985).
[22] S. E. Korshunov and G. V. Uimin, Phase Transitions in Two-Dimensional Uniformly Frustrated XY Models. I. Antiferromagnetic Model on a Triangular Lattice, *J. Stat. Phys.* **43**, 1 (1986).
[23] S. E. Korshunov, Phase Transitions in Two-Dimensional Uniformly Frustrated XY Models. II. General Scheme, *J. Stat. Phys.* **43**, 17 (1986).
[24] E. Granato, Domain Wall Induced XY Disorder in the Fully Frustrated XY Model, *J. Phys. C: Solid State Phys.* **20**, L215 (1987).
[25] P. Minnhagen, Nonuniversal Jumps and the Kosterlitz-Thouless Transition, *Phys. Rev. Lett.* **54**, 2351 (1985).
[26] P. Minnhagen, Empirical Evidence of a Nonuniversal Kosterlitz-Thouless Jump for Frustrated Two-Dimensional XY Models, *Phys. Rev. B* **32**, 7548 (1985).
[27] M. Y. Choi and S. Doniach, Phase Transitions in Uniformly Frustrated XY Models, *Phys. Rev. B* **31**, 4516 (1985).
[28] M. Yosefin and E. Domany, Phase Transitions in Fully Frustrated Spin Systems, *Phys. Rev. B* **32**, 1778 (1985).
[29] M. Y. Choi and D. Stroud, Critical Behavior of Pure and Diluted XY Models with Uniform Frustration, *Phys. Rev. B* **32**, 5773 (1985).
[30] E. Granato and J. M. Kosterlitz, Critical Behavior of Coupled XY Models, *Phys. Rev. B* **33**, 4767 (1986).
[31] J. M. Thijssen and H. J. F. Knops, Monte Carlo Transfer-Matrix Study of the Frustrated XY Model, *Phys. Rev. B* **42**, 2438 (1990).
[32] J. Y. Lee, J. M. Kosterlitz and E. Granato, Monte Carlo Study of Frustrated XY Models on a Triangular and Square Lattice, *Phys. Rev. B* **43**, 11531 (1991).
[33] G. Ramirez-Santiago and J. V. José, Correlation Functions in the Fully Frustrated 2D XY Model, *Phys. Rev. Lett.* **68**, 1224 (1992).
[34] G. Ramirez-Sanitago and J. V. José, Critical Exponents of the Fully Frustrated Two-Dimensional XY Model, *Phys. Rev. B* **49**, 9567 (1994).
[35] E. Granato and M. P. Nightingale, Chiral Exponents of the Square-Lattice Frustrated XY Model: A Monte Carlo Transfer-Matrix Calculation, *Phys. Rev. B* **48**, 7438 (1993).
[36] S. Y. Lee and K. C. Lee, Phase Transitions in the Fully Frustrated XY Model Studied with Use of the Microcanonical Monte Carlo Technique, *Phys. Rev. B* **49**, 15184 (1994).
[37] P. Olsson, Two Phase Transitions in the Fully Frustrated XY Model, *Phys. Rev. Lett.* **75**, 2758 (1995). Olsson
[38] P. Olsson, Olsson Replies: Two Phase Transitions in the Fully Frustrated XY Model, *Phys. Rev. Lett.* **77**, 4850 (1996).
[39] P. Olsson, Monte Carlo Study of the Villain Version of the Fully Frustrated XY Model, *Phys. Rev. B* **55**, 3585 (1997).
[40] V. Cataudella and M. Nicodemi, Efficient Cluster Dynamics for the Fully Frustrated XY Model, *Physica A* **233**, 293 (1996).
[41] E. H. Boubcheur and H. T. Diep, Critical Behavior of the Two-Dimensional Fully Frustrated XY Model, *Phys. Rev. B* **58**, 5173 (1998).
[42] Y. Ozeki and N. Ito, Nonequilibrium Relaxation Analysis of Fully Frustrated XY Models in Two Dimensions, *Phys. Rev. B* **68**, 054414 (2003).
[43] D. H. Lee, J. D. Joannopoulos, J. W. Negele and D. P. Landau, Discrete Symmetry Breaking and Novel Critical Phenomena in an Antiferromagnetic Planar (XY) Model in Two Dimensions, *Phys. Rev. Lett.* **52**, 433 (1984).
[44] D. H. Lee, J. D. Joannopoulos, J. W. Negele and D. P. Landau, Symmetry Analysis and Monte Carlo Study of a Frustrated Antiferromagnetic Planar (XY) Model in Two

Dimensions, *Phys. Rev. B* **33**, 450 (1986).
[45] S. Miyashita and H. Shiba, Nature of the Phase Transition of the Two-Dimensional Antiferromagnetic Pland Rotator Model on the Triangular Lattice, *J. Phys. Soc. Jpn.* **53**, 1145 (1984).
[46] W. Y. Shih and D. Stroud, Superconducting Arrays in a Magnetic Field: Effects of Lattice Structure and a Possible Double Transition, *Phys. Rev. B* **30**, 6774 (1984).
[47] J. E. Van Himbergen, Monte Carlo Study of a Generalized-Planar-Model Antiferromagnet with Frustration, *Phys. Rev. B* **33**, 7857 (1986).
[48] H.-J. Xu and B. W. Southern, Phase Transitions in the Classical XY Antiferromagnet on the Triangular Lattice, *J. Phys. A: Math. Gen.* **29** L133 (1996).
[49] S. Lee and K. C. Lee, Phase Transitions in the Fully Frustrated Triangular XY Model, *Phys. Rev. B* 57, 8472 (1998).
[50] J. D. Noh, H. Rieger, M. Enderie and K. Knorr, Critical Behavior of the Frustrated Antiferromagnetic Six-State Clock Model on a Triangular Lattice, *Phys. Rev. E* **66**, 026111 (2002).
[51] G. S. Grest, Critical Behavior of the Two-Dimensional Uniformly Frustrated Charged Coulomb Gas, *Phys. Rev. B* **39**, 9267 (1989).
[52] J. M. Thijssen and H. J. F. Knops, Monte Carlo Study of the Coulomb-Gas Representation of Frustrated XY Models, *Phys. Rev. B* **37**, 7738 (1988).
[53] J. M. Thijssen, Phase Diagram of the Frustrated XY Model on a Triangular Lattice, *Phys. Rev. B* **40**, 5211 (1989).
[54] J.-R. Lee, Phase Transitions in the Two-Dimensional Classical Lattice Coulomb Gas of Half-Integer Charges, *Phys. Rev. B* **49**, 3317 (1994).
[55] B. Berg, H. T. Diep, A. Ghazali and P. Lallemand, Phase Transitions in Two-Dimensional Uniformly Frustrated XY Spin Systems, *Phys. Rev. B* **34**, 3177 (1986).
[56] E. Granato and J. M. Kosterlitz, Frustrated XY Model with Unequal Ferromagnetic and Antiferromagnetic Bonds, *J. Phys. C: Solid State Phys.* **19**, L59 (1986).
[57] E. Granato, J. M. Kosterlitz, J. Y. Lee and M. P. Nightingale, Phase Transitions in Coupled XY-Ising Systems, *Phys. Rev. Lett.* **42**, 1090 (1991)
[58] J. Y. Lee, E. Granato and J. M. Kosterlitz, Nonuniversal Critical Behavior and First-Order Transitions in a Coupled XY-Ising Model, *Phys. Rev. B* **44**, 4819 (1991).
[59] M. P. Nightingale, E. Granato and J. M. Kosterlitz, Conformal Anomaly and Critical Exponents of the XY Ising Model, *Phys. Rev. B* **52**, 7402 (1994).
[60] G. Cristofano, V. Marotta, P. Minnhagen, A. Naddeo and G. Niccoli, CFT Description of the Fully Frustrated XY Model and Phase Diagram Analysis, *J. Stat. Mech. Theo. and Expt.*, P11009 (2006).
[61] P. Minnhagen, B. J. Kim, S. Bernhardsson and G. Cristofano, Phase Diagram of Generalized Fully Frustrated XY Model in Two Dimensions, *Phys. Rev. B* **76**, 224403 (2007).
[62] P. Minnhagen, B. J. Kim, S. Bernhardsson and G. Cristofano, Symmetry-Allowed Phase Transitions Realized by the Two-Dimensional Fully Frustrated XY Class, *Phys. Rev. B* **78**, 184432 (2008).
[63] P. Minnhagen, S. Bernhardsson and B. J. Kim, The Groundstates and Phases of the Two-Dimensional Fully Frustrated XY Model, *Int'l. J. Mod. Phys. B* **23**, 2929 (2009).
[64] M. Hasenbusch, A. Pelissetto and E. Vicari, Transitions and Crossover Phenomena in Fully Frustrated XY Systems, *Phys. Rev. B* **72**, 184502 (2005).
[65] M. Hasenbusch, A. Pelissetto and E. Vicari, Multicritical Behavior in the Fully Frustrated XY Model and Related Systems, *J. Stat. Mech: Theo. and Expt.* P12002 (2005).
[66] S. Okumura, H. Yoshino and H. Kawamura, Spin-Chirality Decoupling and Critical Properties of a Two-Dimensional Fully Frustrated XY Model, *Phys. Rev. B* **83**, 094429

(2011).
[67] S. E. Korshunov, Kink Pairs Unbinding on Domain Walls and the Sequence of Phase Transitions in the Fully Frustrated XY Models, *Phys. Rev. Lett.* **88**, 167007 (2002).
[68] The unbinding transition of logarithmically interacting charges in one dimension was first discussed in: S. A. Bulgadaev, Phase Transitions in Gases with Generalized Charges, *Phys. Lett. A* **86**, 213 (1981); Phase Transitions in Gases with Generalized Charges Interacting Through a Logartithmic Law. 2. $D = 1$, Isotropic Case, *Teor. Mat. Fiz.* **51**, 424 (1982) [*Theor. Math. Phys.* **51**, 593 (1982)].
[69] P. Olsson and S. Teitel, Kink-Antikink Unbinding Transition in the Two-Dimensional Fully Frustrated XY Model, *Phys. Rev. Lett.* **71**, 104423 (2005).
[70] J.-R. Lee and S. Teitel, Phase Transitions in Classical Two-Dimensional Lattice Coulomb Gases, *Phys. Rev. B* **46**, 3247 (1992).
[71] V. Gotcheva, Y. Wang, A. T. J. Wang, and S. Teitel, Continuous-Time Monte Carlo and Spatial Ordering in Driven Lattice Gases: Application to Driven Vortices in Periodic Superconducting Networks, *Phys. Rev. B* **72**, 064505 (2005).
[72] S. E. Korshunov and B. Douçot, Fluctuations and Vortex-Pattern Ordering in the Fully Frustrated XY Model on a Honeycomb Lattice, *Phys. Rev. Lett.* **93**, 097003 (2004)
[73] S. E. Korshunov, Vortex Ordering in Fully Frustrated Superconducting Systems with a Dice Lattice, *Phys. Rev. B* **63**, 134503 (2001).
[74] S. E. Korshunov, Fluctuation-Induced Vortex Pattern and its Disordering in the Fully Frustrated XY Model on a Dice Lattice, *Phys. Rev. B* **71**, 174501 (2005).
[75] C. Denniston and C. Tang, Domain Walls and Phase Transitions in the Frustrated Two-Dimensional XY Model, *Phys. Rev. Lett.* **79**, 451 (1997).
[76] C. Denniston and C. Tang, Low-Energy Excitations and Phase Transitions in the Frustrated Two-Dimensional XY Model, *Phys. Rev. B* **58**, 6591 (1998).
[77] M. Kolahchi and J. P. Straley, Ground State of the Uniformly Frustrated Two-Dimensional XY Model Near $f = 1/2$, *Phys. Rev. B* **43**, 7651 (1991).
[78] M. Franz and S. Teitel, Vortex-Lattice Melting in Two-Dimensional Superconducting Networks and Films, *Phys. Rev. B* **51**, 6551 (1995).
[79] V. Gotcheva and S. Teitel, Depinning Transition of a Two-Dimensional Vortex Lattice in a Commensurate Periodic Potential, *Phys. Rev. Lett.* **86**, 2126 (2001).
[80] S. E. Korshunov, A. Vallat, and H. Beck, Frustrated XY models with Accidental Degeneracy of the Ground State, *Phys. Rev. B* **51**, 3071 (1995).
[81] T. C. Halsey, Josephson-Junction Array in an Irrational Magnetic Field: A Superconducting Glass?, *Phys. Rev. Lett.* **55**, 1018 (1985).
[82] P. Gupta, S. Teitel, and M. J. P. Gingras, Glassiness Versus Order in Densely Frustrated Josephson Arrays, *Phys. Rev. Letts.* **80**, 105 (1998).
[83] C. Denniston and C. Tang, Incommensurability in the Frustrated Two-Dimensional XY Model, *Phys. Rev. B* **60**, 3163 (1999).
[84] M. R. Kolahchi and H. Fazli, Behavior of a Josephson-Junction Array with Golden Mean Frustration, *Phys. Rev. B* **62**, 9089 (2000).
[85] S. Y. Park, M. Y. Choi, B. J. Kim, G. S. Jeon, and J. S. Chung, Intrinsic Finite-Size Effects in the Two-Dimensional XY Model with Irrational Frustration, *Phys. Rev. Lett.* **85**, 3484 (2000).
[86] E. Granato, Zero-Temperature Resistive Transition in Josephson-Junction Arrays at Irrational Frustration, *Phys. Rev. B* **75**, 184527 (2007).
[87] E. Granato, Phase and Vortex Correlations in Superconducting Josephson-Junction Arrays at Irrational Magnetic Frustration, *Phys. Rev. Lett.* **101**, 027002 (2008).
[88] J. P. Straley and G. M. Barnett, Phase diagram for a Josephson network in a magnetic

field, *Phys. Rev. B* **48**, 3309 (1993).

[89] M. R. Kolahchi, Finding Local Minimum States of Josephson-Junction Arrays in a Magnetic Field, *Phys. Rev. B* **56**, 95 (1997).

[90] M. R. Kolahchi, Ground State of Uniformly Frustrated Josephson-Junction Arrays at Irrational Frustration, *Phys. Rev. B* **59**, 9569 (1999).

[91] S. J. Lee, J.-R. Lee, and B. Kim, Patterns of Striped Order in the Classical Lattice Coulomb Gas, *Phys. Rev. Lett.* **88**, 025701 (2002).